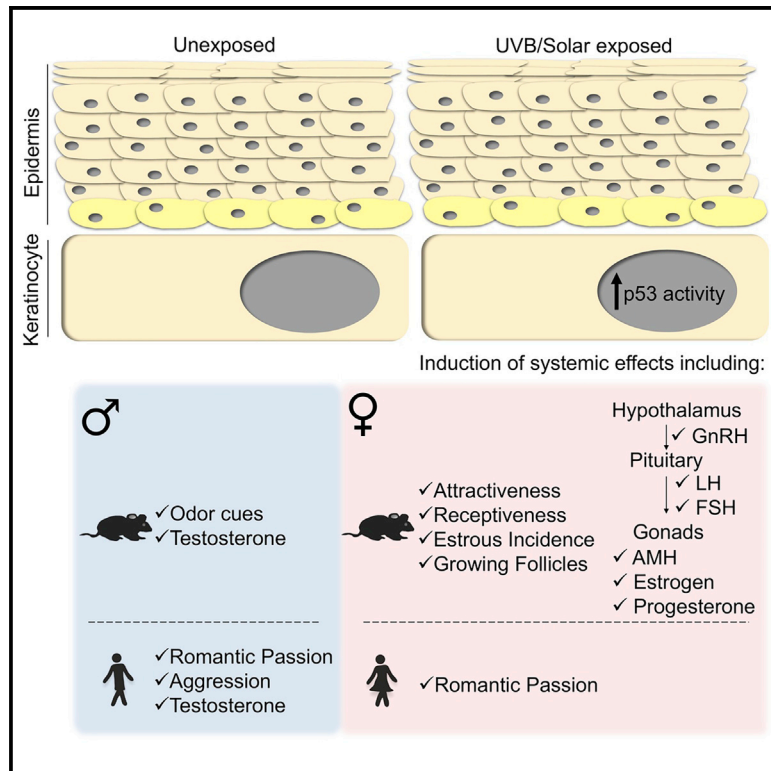# Skin exposure to UVB light induces a skin-brain-gonad axis and sexual behavior

Graphical abstract

Authors

Roma Parikh, Eschar Sorek, Shivang Parikh, ..., Ruth Percik, Aron Weller, Carmit Levy

Correspondence

carmitlevy@post.tau.ac.il

In brief

Parikh et al. find that UVB exposure triggers a skin-brain-gonadal axis through skin p53 activation. UVB exposure increases in female mice sexual responsiveness and attractiveness, hypothalamus-pituitary-gonadal axis hormone levels, ovary size, and estrus duration, as well as male-female interactions. Solar exposure in humans enhances romantic passion and positively correlates with male testosterone levels.

Highlights

- UVB exposure increases circulating sex-steroid levels in mice and humans

- UVB exposure enhances female attractiveness and receptiveness toward males

- UVB exposure increases females' estrus phase, HPG axis hormones, and follicle growth

- Skin p53 regulates UVB-induced sexual behavior and ovarian physiological changes

CellPress

Article

Skin exposure to UVB light induces a skin-brain-gonad axis and sexual behavior

Roma Parikh,[1] Eschar Sorek,[1] Shivang Parikh,[1] Keren Michael,[2] Lior Bikovski,[3,4] Sagi Tshori,[5,6] Galit Shefer,[5] Shira Mingelgreen,[5] Taiba Zornitzki,[7] Hilla Knobler,[7] Gabriel Chodick,[8,23] Mariya Mardamshina,[1] Arjan Boonman,[9] Noga Kronfeld-Schor,[9] Hadas Bar-Joseph,[10] Dalit Ben-Yosef,[11,12] Hadar Amir,[13,14] Mor Pavlovsky,[15] Hagit Matz,[15,16] Tom Ben-Dov,[1,17] Tamar Golan,[1] Eran Nizri,[15,16] Daphna Liber,[18] Yair Liel,[19] Ronen Brenner,[20] Yftach Gepner,[21] Orit Karnieli-Miller,[22] Rina Hemi,[23] Ruth Shalgi,[24] Tali Kimchi,[25] Ruth Percik,[16,23] Aron Weller,[26] and Carmit Levy[1,27,*]

[1]Department of Human Genetics and Biochemistry, Sackler Faculty of Medicine, Tel Aviv University, Tel Aviv 69978, Israel
[2]Department of Human Services, The Max Stern Yezreel Valley Academic College, Jezreel Valley 1930600, Israel
[3]The Myers Neuro-Behavioral Core Facility, Sackler School of Medicine, Tel Aviv University, Tel Aviv 69978, Israel
[4]School of Behavioral Sciences, Netanya Academic College, Netanya 4223587, Israel
[5]Research Authority, Kaplan Medical Center, Rehovot, Israel
[6]Department of Biochemistry and Molecular Biology, Institute for Medical Research Israel-Canada, The Hebrew University, Jerusalem, Israel
[7]Diabetes, Endocrinology and Metabolic Disease Institute, Kaplan Medical Center, Hadassah School of Medicine, Hebrew University in Jerusalem, Rehovot, Israel
[8]Maccabitech, Maccabi Healthcare Services, Tel Aviv, Israel
[9]School of Zoology, Faculty of Life Sciences and the Sagol School of Neuroscience, Tel Aviv University, Tel Aviv 6997801, Israel
[10]The TMCR Unit, Sackler Faculty of Medicine, Tel Aviv University, Tel Aviv 69978, Israel
[11]IVF Lab & Wolfe PGD-Stem Cell Lab, Fertility Institute, Tel Aviv Sourasky Medical Center, Tel Aviv, Israel
[12]Department of Cell Biology and Development, Sackler Faculty of Medicine & Sagol School of Neuroscience, Tel Aviv University, Tel Aviv, Israel
[13]Fertility Institute, Tel Aviv Sourasky Medical Center, Tel Aviv, Israel
[14]Sackler Faculty of Medicine, Tel Aviv University, Tel Aviv, Israel
[15]Department of Dermatology, Tel Aviv Sourasky (Ichilov) Medical Center, Tel Aviv 6423906, Israel
[16]Sackler School of Medicine, Tel Aviv University, Tel Aviv 69978, Israel
[17]Department of Otolaryngology, Head and Neck surgery, Meir Medical Center, Kfar Saba 4428164, Israel
[18]Faculty of Humanities, Education and Social Sciences, Ono Academic College, Kiryat Ono, Israel
[19]Faculty of Health Sciences, Ben-Gurion University of the Negev, Beer-Sheva, Israel
[20]Institute of Pathology, E. Wolfson Medical Center, Holon 58100, Israel
[21]School of Public Health, Sackler Faculty of Medicine and Sylvan Adams Sports Institute, Tel Aviv University, Tel Aviv 69978, Israel
[22]Department of Medical Education, Sackler Faculty of Medicine, Tel Aviv University, Tel Aviv 69978, Israel
[23]Institute of Endocrinology, Chaim Sheba Medical Center, Tel-Hashomer, Israel
[24]Department of Cell and Developmental Biology, Sackler Faculty of Medicine, Tel Aviv University, Tel Aviv 69978, Israel
[25]Department of Neurobiology, Weizmann Institute of Science, Rehovot, Israel
[26]Department of Psychology and the Gonda Brain Research Center, Bar-Ilan University, Ramat Gan 5290002, Israel
[27]Lead contact
*Correspondence: carmitlevy@post.tau.ac.il
https://doi.org/10.1016/j.celrep.2021.109579

SUMMARY

Ultraviolet (UV) light affects endocrinological and behavioral aspects of sexuality via an unknown mechanism. Here we discover that ultraviolet B (UVB) exposure enhances the levels of sex-steroid hormones and sexual behavior, which are mediated by the skin. In female mice, UVB exposure increases hypothalamus-pituitary-gonadal axis hormone levels, resulting in larger ovaries; extends estrus days; and increases anti-Mullerian hormone (AMH) expression. UVB exposure also enhances the sexual responsiveness and attractiveness of females and male-female interactions. Conditional knockout of p53 specifically in skin keratinocytes abolishes the effects of UVB. Thus, UVB triggers a skin-brain-gonadal axis through skin p53 activation. In humans, solar exposure enhances romantic passion in both genders and aggressiveness in men, as seen in analysis of individual questionaries, and positively correlates with testosterone level. Our findings suggest opportunities for treatment of sex-steroid-related dysfunctions.

INTRODUCTION

Exposure to the ultraviolet (UV) component of solar radiation increases testosterone levels in men (Myerson and Neustadt, 1939), estradiol and testosterone levels in fish (Mitchell et al., 2014), and the attractiveness of hens to cockerels (Jones et al., 2001). This suggests that exposure to UV plays a major role in the regulation of sexuality on both behavioral and endocrinological

levels. The mechanism underlying this effect remains poorly understood.

The reproductive endocrine system includes organs such as the hypothalamus, pituitary, thyroid, pineal and adrenal glands, ovaries, and testes (Rawindraraj et al., 2019). The system is governed by the hypothalamus, which sends signaling mediators such as gonadotropin-releasing hormone (GnRH) to the pituitary gland to induce release of follicle-stimulating hormone (FSH) and luteinizing hormone (LH). In turn, these hormones transmit signals to the male and female gonads (Rawindraraj et al., 2019), the testicles and the ovaries, respectively, promoting sex-steroid production and gametogenesis (Rawindraraj et al., 2019). In females, FSH and LH stimulate the production of estrogen and progesterone, which regulate ovulation and pregnancy (Barbieri, 2014; Rosner and Sarao, 2019). In most female mammals, sexual activity and receptivity are confined to the preovulatory period (Wallner et al., 2019) and the estrus phase (Kim et al., 2016) of the menstrual/estrous cycle. These cyclic hormonal changes dictate sexual behavior. In humans, it has been shown that men respond more favorably to a woman's scent (Kuukasjärvi et al., 2004) or facial appearance (Roberts et al., 2004) during the preovulatory phase of the woman's cycle.

The skin, consisting of epidermal, dermal, and hypodermal layers, is the largest body organ (Golan et al., 2015; Yousef et al., 2020). In contrast to the vast literature on the skin as a hormonal target (Slominski and Wortsman, 2000; Zouboulis, 2004), its role as a source of hormones is less understood. The skin is capable of producing and releasing hormones including vitamin D, various peptides derived from proopiomelanocortin (POMC), β-endorphin (Fell et al., 2014), and corticotropin-releasing hormone (CRH) (Skobowiat and Slominski, 2015), resembling the central regulatory paradigms of the hypothalamic-pituitary-adrenal axis (Slominski and Wortsman, 2000; Slominski et al., 2015). β-endorphin release into the circulation is implicated in sun-addiction behavior (Fell et al., 2014). Furthermore, ultraviolet B (UVB) exposure is linked to increased expression of the stress-response hormone CRH, as well as with components of the hypothalamus-pituitary-adrenal (HPA) axis, including adrenocorticotropic hormone (ACTH) and corticosterone, both in the skin and in the plasma; stimulation of corticosterone production was seen in the absence of pituitary involvement (Skobowiat and Slominski, 2015; Skobowiat et al., 2011, 2017; Slominski et al., 2013, 2018). These data situate the skin as an important component in the regulation of stress-related behaviors and sun-addiction behavior.

Given that the furless human skin contacts the environment in general and the sun's rays in particular, it is conceivable that the skin plays a role in hormone-related social, sexual, and reproductive behavior, but this assumption has yet to be verified. Solar radiation (bright light and radiant heat) from the sun includes infrared, visible, and UV. UV light is further divided into UVA, UVB, and UVC (Hölzle and Hönigsmann, 2005). Here, we report, using behavioral tests in mice, that UVB treatment significantly enhanced the sexual responsiveness of females, which in turn increases male sexual arousal and behavior. Furthermore, UVB treatment significantly enhanced the desire for male-female interaction and female attractiveness to males. In terms of physiological changes, we found that UVB treatment increased the incidence of estrus days

and enhanced ovary size and anti-Mullerian hormone (AMH) expression in mice. Mechanistically, we demonstrated that the UVB-induced sexual behavior and hormonal changes are mediated by p53 activation in epidermal keratinocytes through a skin-brain-gonadal axis. We also demonstrated, using questionnaires, that UVB treatment enhanced romantic passion in both men and women and aggressiveness in men and is positively correlated with testosterone level. This study suggests that UVB phototherapy has potential as an ancillary treatment of sex-steroid-related dysfunctions.

RESULTS

Daily UVB treatment enhances female sexual attractiveness and receptiveness

To investigate the systemic effects of UVB radiation, we exposed dorsally shaved mice to a single UVB dose of 800 mJ/cm^2 (Svobodová et al., 2012) or to 50 mJ/cm^2 daily for 8 weeks, a sub-erythemic UVB dose that is equivalent to 20–30 min of midday sun (Fell et al., 2014). Blood samples were collected 24 h after UVB treatment for the acute model and after 8 weeks of UVB treatment for chronic models (Figure S1A). As expected (Malcov-Brog et al., 2018), skin pigmentation increased in the tails of both male and female mice upon chronic exposure compared with mock treatment (control) (Figure S1B). Furthermore, we found significant positive activation Z score for upstream regulators β-estradiol, testosterone, and estrogen in male mice (Figure 1A, right panel) and for estrogen, androgen, β-estradiol, and progesterone in female mice after chronic UVB treatment compared with the controls (Figure 1A, right panel). Acute exposure of mice did not result in significant activation of sex-steroid signaling (Figure S1C), suggesting that the chronic dose of UVB exposure is a more physiologically relevant model. Sex steroids released from gonads activate the neuronal pathways involved in sexual behavior in zebrafish (Pradhan and Olsson, 2015), and testosterone injections enhance mounting behavior in males by priming the neural tissues mediating the mating behavior in guinea pigs (Phoenix et al., 1959). These data suggest that UVB treatment enhances sex-steroid signaling in both male and female mice and thus might influence mating behavior.

Mating behavior in rodents consists of several behaviors. Attractivity (Beach, 1976) involves efforts to elicit a response from the opposite sex by vocalizations and olfactory and visual stimuli (Beach, 1976). Proceptivity includes estrus responsiveness and purposive vocalizations (Beach, 1976), and female receptivity involves lordosis behavior that involves readiness to be involved in copulation, which culminates in successful intromission (Beach, 1976). To assess the effect of UVB on reproductive behavior, we conducted a mating test (Figure 1B) in which a sexually naive female, either UVB treated or mock treated (control), was introduced into the home cage of a sexually naive male that had been UVB treated or mock treated (control). Sexual receptivity in rodents varies with the stage of the female estrous cycle (Zinck and Lima, 2013). To exclude the differences in female sexual receptivity, we evaluated the estrous cycle of the female by vaginal cytology (Caligioni, 2009) and used only females in the estrus/proestrus stage for the mating test. During the 1-h mating test, we monitored vocalization, sniffing, self-grooming,
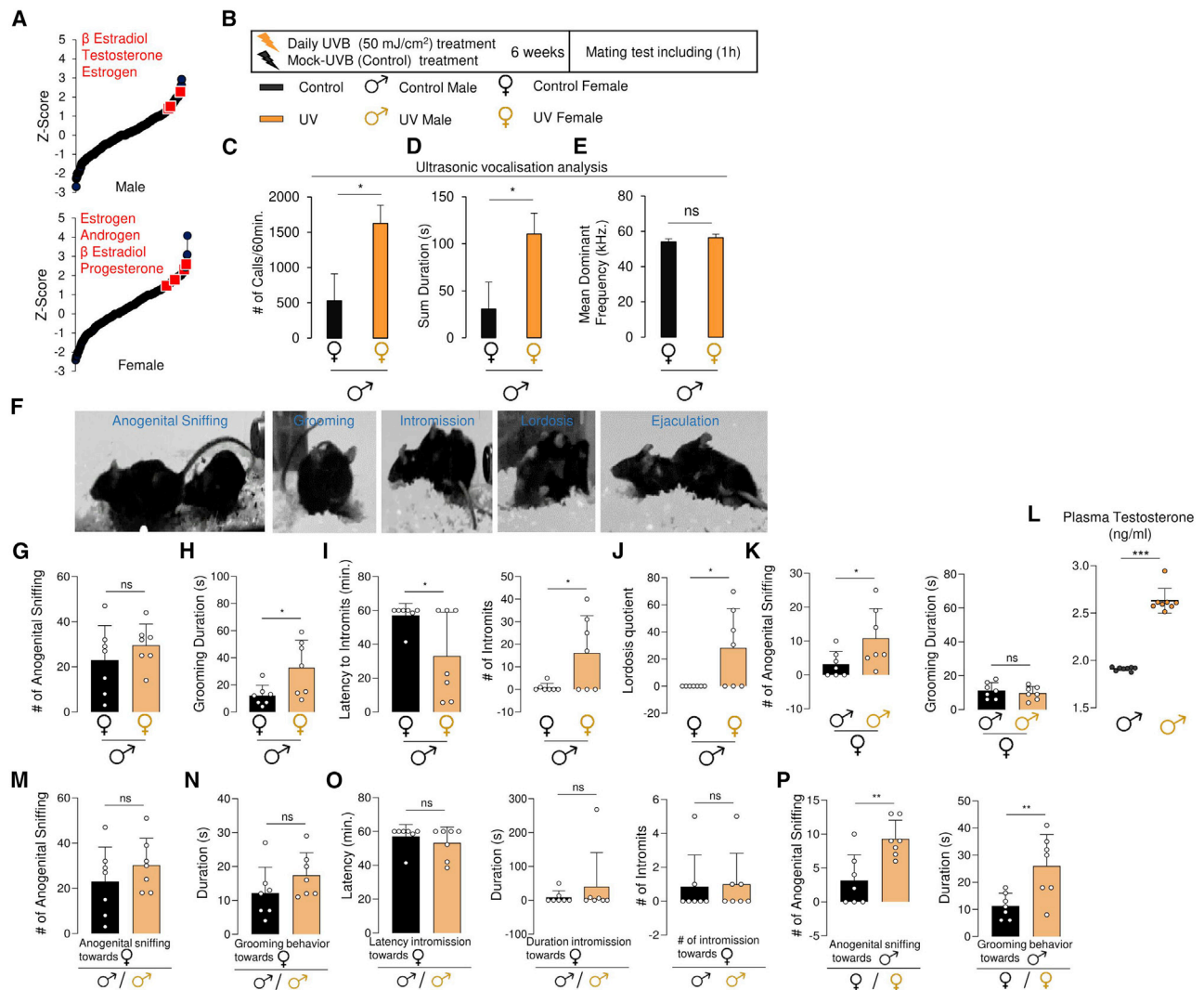
Figure 1. Daily UVB treatment enhances female sexual attractiveness and receptiveness

(A) Activation *Z* scores of predicted upstream regulators of mice upon UVB treatment for 6 weeks.

(B) Schematic representation of the mating test with male and female mice treated with UVB or control for 6 weeks.

(C–E) Total number, total time, and mean dominant frequency of USVs by control males in the presence of UVB- or control-treated females.

(F) Representative photograph of sexual behavior parameters.

(G) Total number of control male anogenital sniffing events of UVB- or control-treated females.

(H) Total time self-grooming by control males in the presence of UVB- or control-treated females.

(I) Latency intromission (left) and total number of intromissions (right) by control males on UVB- or control-treated females.

(J) UVB- or control-treated females' lordosis quotient upon control male mounting.

(K) Total number of anogenital sniffing events (left) and total time self-grooming (right) for control females in the presence of UVB- or control-treated males.

(L) Plasma testosterone levels of males upon 8 weeks of UVB or control treatment.

(M) Total number of anogenital sniffing events by UVB- or control-treated males on a control-treated female.

(N) Total time spent self-grooming by UVB- or control-treated males for a control-treated female.

(O) Latency intromission (left panel), duration of intromission (middle panel), and total number of intromissions (right panel) by a UVB- or control-treated male on a control female.

(P) Total number of anogenital sniffing events (left) and total time self-grooming (right) by UVB- or control-treated females on a control-treated male.

Data are means ± SEM, n = 3 (A and C–E), n = 7 (G–K and M–P), n = 8 (L). For data analysis, a two-tailed, unpaired Student's t test was performed. *p < 0.05; **p < 0.01; ***p < 0.001; ns, not statistically significant.

intromission, lordosis, and ejaculation as has been done previously (Achiraman et al., 2014; Beach, 1976; Haga et al., 2010; Kimchi et al., 2007).

To determine the effect of UVB exposure on attractivity, we assessed ultrasonic vocalizations (USVs) (Costantini and D'Amato, 2006). During a male-female encounter, male mice exclusively

dominate the calls (frequency of 40–70 kHz), a behavior positively related to their level of sexual arousal (Kerchner, 2004). We evaluated the effect of UVB treatment on the USVs of control males in the presence of a UVB-treated or control female as a stimulus. The audio recordings were then extracted into several parameters, including total call duration and its mean dominant frequency using UltraVox XT 3.1 software. The total number of control male calls (Figure 1C; Figure S1D) and their total duration (Figure 1D) were significantly higher when males were matched with UVB-treated females than with control females. There was no difference in frequencies of the calls with the highest energy (mean dominant frequency) (Figure 1E), indicating that the duration and number of calls changed but the type of call did not. These results suggest that UVB treatment of females enhances their attractivity as indicated by the relative increase in male vocalization parameters.

Next, we evaluated the effect of UVB treatment on female attractiveness by measuring anogenital sniffing behavior (Clarke and Trowill, 1971) (Figure 1F; Video S1). Males exhibited similar sniffing behavior during the 1-h test session regardless of the treatment the female received (Figure 1G). Self-grooming reflects an attraction to the opposite sex (Achiraman et al., 2014; Haga et al., 2010), and the total duration of grooming (Figure 1F; Videos S2A and S2B) was significantly enhanced for males in the presence of UVB-treated females compared with control females (Figure 1H). Furthermore, we analyzed intromission, which is a measurement of a successful mating event by the male on a receptive female (Haga et al., 2010) (Figure 1F; Video S3). The latency to intromit was significantly shorter for UVB-treated than for control females (Figure 1I, left panel). The duration (Figure S1E) and total number of successful intromissions (Figure 1I, right panel) were significantly greater when males were mated with UVB-treated females than with controls. This indicated that males are more attracted to and subsequently sexually more successful with UVB-treated females.

During intromission, the receptiveness of the female is measured by her lordotic response (Haga et al., 2010) (Figure 1F; Video S3). We found a significant increase in the lordosis quotient of UVB-treated females toward males compared with that exhibited by mock-treated females (Figure 1K), suggesting that UVB enhances female receptiveness. No change was observed in the rearing behavior of females (Figure S1F), indicating no difference in forced intromission encounters.

Finally, male ejaculation did not significantly differ between UVB- or mock-treated females (Figure 1F; Figure S1G; Video S4). Similar tests were performed using UVB-treated males, and differences between the number of ejaculations did not differ when females were UVB or mock treated (Figure S1H). This demonstrates that UVB treatment significantly enhances the attractiveness and responsiveness of female mice, which in turn increases the sexual arousal and behavior of males.

Next, we measured the effect of UVB on male attractiveness by testing anogenital sniffing and grooming of a female in the presence of UVB-treated or control males. Females exhibited significantly more anogenital sniffing events toward UVB-treated males compared with control males (Figure 1K, left panel). No significant difference was observed in female grooming behavior (Figure 1K, right panel). Similar tests were performed using UVB-

treated females, demonstrating same significant trend toward the UVB-treated male compare to control male (Figure S1I), suggesting an increase in male odor upon UVB exposure.

Because testosterone is involved in synthesis and secretion of pheromones (Asaba et al., 2014), male attractivity (Mitra and Sapolsky, 2012; Schellino et al., 2016), and social and emotional bonds with females (van der Meij et al., 2012), we found significantly higher plasma total testosterone levels in UVB- than mock-treated male mice (Figure 1L). We found no change in the level of testosterone in female mice upon UVB exposure (Figure S1J).

Next, we tested the effect of UVB treatment on the social/sexual behavior of males and females. No significant differences were observed in anogenital sniffing, grooming behavior, latency to intromit, duration of intromission, and number of intromissions by control or UVB-treated male mice mated with control-treated females (Figures 1M–1O). However, UVB treatment significantly increased female anogenital sniffing and grooming behavior toward control males (Figure 1P). This suggests that UVB treatment enhances social/sexual behavior of females. Because grooming behavior is also a known characteristic of anxiety in rodents (Kalueff et al., 2016), we evaluated anxiety in an elevated plus maze test, a classic measure of anxiety-related behavior (Walf and Frye, 2007). Our results demonstrate that males treated with UVB displayed a significant reduction in their anxiety level compared with the control males (Figure S1K), as was shown previously for male mice (Fell et al., 2014). No difference was observed in the anxiety levels of females (Figure S1L). These data support our conclusion that an increase in grooming behavior might be indicative of attraction to the opposite sex irrespective of anxiety. Altogether, our data demonstrate that UVB exposure enhances female attraction, the testosterone level in males, and the social/sexual behavior of females.

UVB treatment enhances male and female sexual behavior and female attraction

Sexual selection is based on the preference for social proximity to an attractive partner (Puts, 2010). Given our findings that UVB treatment significantly increases the attractiveness of males and females, we investigated odor-triggered preferences and mate selection through social proximity using the three-chamber test (Yang et al., 2011), in which a subject's preference for one of two stimuli is monitored (Figure 2A). The subject was a UVB- or mock-treated male or female mouse, and the stimulus was a UVB- or mock-treated male, a control female mouse, or a novel object. The wire cages in this test setup ensure that the social behavioral analysis is limited to the subject mouse (Yang et al., 2011). This setup allows olfactory, auditory, and visual stimuli. All females were in the estrus/proestrus stage.

We found that when the stimulus was a UVB-treated or a mock-treated control female mouse, the males exhibited a clear preference for the UVB-treated female (Figure 2B). We analyzed our results in terms of the latency of the subject mouse to venture into a stimulus compartment, the frequency of visits, and the visit duration. Our analysis showed that it took significantly less time for the male to move near the wire cage (Figure 2C, left panel) or into the zone of the wire cage (Figure S2A, left panel) of a UVB-treated female than a mock-treated control female. Furthermore,
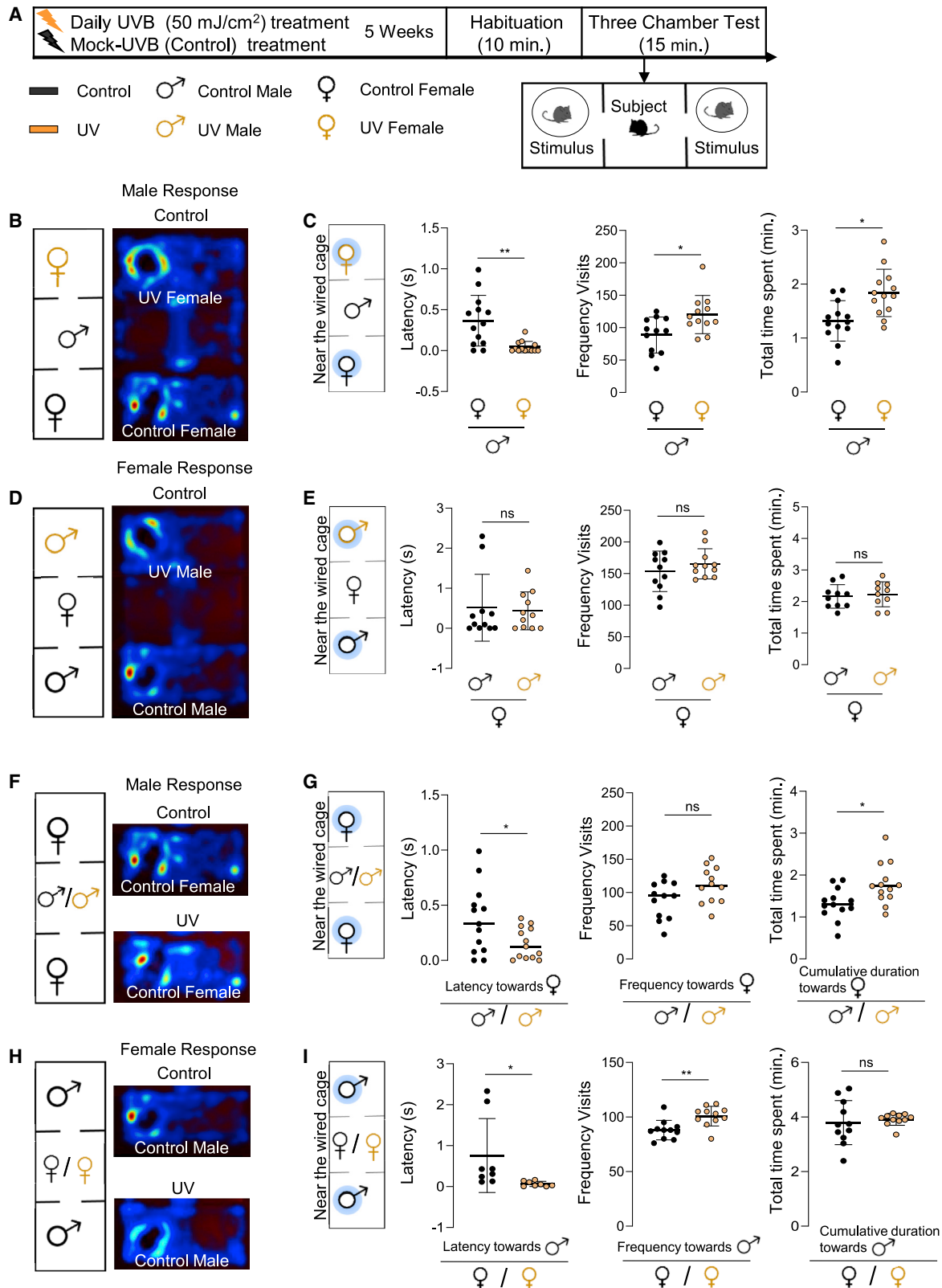
(legend on next page)

the subject males preferred to visit and stay near the wire cage (Figure 2C, middle and right panels) and in the zone of the wire cage (Figure S2A, middle and right panels) of a UVB-treated female rather than a control female. Similar trends of attraction toward the UVB-treated female were observed when the subject was a UVB-treated male (Figures S2B and S2C). These data demonstrate a significant male preference for social proximity to UVB-treated females, supporting our hypothesis that UVB treatment enhances female attractiveness.

Next, we examined the effect of UVB on male attractiveness. The subject female demonstrated no difference in the latency to visit, the frequency of visits, or the total time spent near or in the zone of a wire cage containing a UVB-treated or a mock-treated male stimulus (Figures 2D and 2E; Figure S2D). Similar trends were observed when the subject was UVB-treated female except in a few parameters (Figures S2E and S2F), which might be a result of an interaction between two UVB-treated animals.

Next, to check the effect of UVB on social behavior, we determined the latency to visit, the frequency of visits, and the total time spent by UVB-treated or mock-treated males with a mock-treated control female. We found a significant decrease in the latency to visit and a significant increase in the total time spent near the female by the UVB-treated male subjects compare to the control male subjects (Figures 2F and 2G). No difference was observed in the frequency to visit the female (Figure 2G, middle panel). This suggests that UVB treatment enhances male social behavior. Furthermore, we observed a significant decrease in the latency to visit and a significant increase in the frequency of visits near a wire cage containing a male by the UVB-treated female subjects compared with the control female subjects (Figures 2H and 2I), although no difference was observed in the total time spent next to a male (Figure 2I, right panel). This suggests that UVB treatment enhances female social behavior.

To rule out the possibility that the results are due to mice pausing in the center of the chamber, we measured the total time spent by the subject mouse in the center of the chamber. Notably, no difference was found between the two male subject groups (Figure S2G) or the two female subject groups (Figure S2H). This confirmed that the observed desire for social proximity in both male and female mice results from the UVB treatment.

To validate that male preference for a UVB-treated female mouse results from sexual signals, we repeated the three-chamber test with a female subject, a UVB-treated female stimulus,

and a mock-treated control female stimulus (Figures S2I–S2L). No variation in the social preference of the female subject was observed (Figures S2I–S2L), supporting our hypothesis that UVB treatment induces female sexual attractiveness to males. We also performed the test with a female as a subject and a male and a novel object (plastic block) as stimuli. The results clearly showed that UVB-treated females preferred to visit and stay near the male rather than near the novel object (Figures S2I and S2M); the mock-treated control female demonstrated no such preference (Figures S2M–S2O). These data support our hypothesis that UVB treatment increases the social behavior of female mice with male mice. Altogether, our observations show that UVB treatment significantly enhances the desire for male-female interaction and significantly increases the attractiveness of female mice.

UVB treatment induces romantic passion in humans

To conduct a controlled study of the effect of UVB treatment in humans, we assembled a cohort of patients who were undergoing phototherapy, which provides a documented dose of UVB exposure. The patients were asked to fill an adapted Passionate Love Scale (PLS) questionnaire (Hatfield and Sprecher, 1986) before the first UVB treatment (time point T1) and 1 month thereafter (time point T2). Dermatosis was not expected to have improved at the 1-month time point (Bae et al., 2017; Cameron et al., 2002); thus, therapeutic success, or lack thereof, should not influence the stress levels of subjects, and there should not have been bias in our questionnaire because of therapeutic efficacy. During this period, patients received a UVB dose (0.1–2.5 J/cm) two or three times a week for 10–12 UVB treatments. The PLS, developed to measure passionate love in intimate relationships, focuses on intense longing for union with the other. We found that the male participants' scores were significantly higher at T2 with respect to obsessive thoughts regarding their loved ones, yearning to know everything about her, and endless desire for affection from her (Table 1). However, they also reported significantly less attraction to that person compared with at T1. Female participants at T2 scored significantly higher when it came to feeling that the person whom they loved most passionately is the perfect romantic partner and experiencing a physical response when touched by that person. Furthermore, because we observed an increase in the level of testosterone following UVB treatment in male mice (Figure 1L) and because testosterone is responsible for sexual and aggressive behavior (Muller, 2017), we asked our human cohort of patients undergoing

Figure 2. UVB treatment enhances male and female sexual behavior and female attraction

(A) Schematic representation of the three chamber test for subject and stimulus mice treated for 5 weeks with UVB or control treatment.

(B) Heatmap paths of a control male subject ($n \geq 10$) toward a UVB- or control-treated female stimulus.

(C) Latency of visit (left), frequency of visits (middle), and total time spent (right) by subject control-treated males toward the wire cage of a UVB- or control-treated female stimulus.

(D) Heatmap paths of a control female subject toward a UVB- or control-treated male stimulus.

(E) As in (C) but for female subject movement toward a UVB- or control-treated male stimulus.

(F) Heatmap as in (B), depicting control or UVB-treated subject male movement toward control female stimuli.

(G) As in (C) but for control or UVB-treated male subject movement toward control female stimuli.

(H) Heatmap as in (B) but for UVB- or control-treated female subject movement toward control male stimuli.

(I) As in (C) but for UVB- or control-treated female subject movement toward control male stimuli.

Data are presented as means ± SEM, $n \geq 10$. For data analysis, a two-tailed, unpaired Student's t test was performed. *$p < 0.05$; **$p < 0.01$; ns, not statistically significant.

Table 1. Within-group differences in passionate love

	Males					Females				
	T1		T2			T1		T2		
	Median	Range	Median	Range	Z	Median	Range	Median	Range	Z
Obsessive thoughts on __ [a]	3	1–7	5	2–7	−1.63[b] *	2	1–8	3	1–6	−0.65[b]
Rather be with __ than anyone else	8	4–9	8	6–9	−0.96[b]	6.5	1–9	7.5	1–9	−0.95[b]
Yearn to know everything on __	7	4–9	8	6–9	−2.06[b] *	5	1–9	5	2–9	−0.86[b]
Endless appetite for affection from __	7	3–9	8	5–9	−1.71[b] *	4.5	1–9	5	1–9	−1.20[b]
__ is the perfect romantic partner	8	4–9	8	1–9	−0.14[b]	7	2–9	8	3–9	−2.00[b] *
Sense body responding when __ touches	9	3–9	8	1–9	−0.32[b]	7	2–9	8.5	3–9	−1.73[b] *
Possess a powerful attraction to __	8	4–9	7	1–9	−1.89[c] *	7	2–9	7	2–9	−0.32[b]

*p < 0.05; **p < 0.01.
[a]__, name of the person whom the participant loved most passionately.
[b]Based on negative ranks.
[c]Based on positive ranks.

phototherapy to complete an aggression questionnaire (Buss and Perry, 1992) at T1 and T2. Our results indicate that male participants were significantly more verbally aggressive at T2 than at T1 (Table S1), whereas women showed no difference. Neither men nor women had a significant change in the level of physical aggression between T1 and T2. Altogether, our data suggest that in humans, UVB treatment enhances passionate love in both genders and increases some aspects of aggressiveness in men.

UVB treatment increases estrus incidence and the number of growing follicles

UVB treatment was found to enhance female sexual/social behavior, receptiveness, and attractiveness in mice, so we investigated its effect on the estrus phase, because females are more sexually receptive and attractive during its estrus stage (Kim et al., 2016). To this end, we followed the estrous cycle of eight female mice for 45 days using the vaginal smear method (Caligioni, 2009) (Figure S3A). We found a significant increase in the percentage of estrus days from the total number of 45 tested days (Figure 3A) and in the length of the estrus phase (Figure 3B) in UVB-treated females. These data suggest that UVB treatment modifies the estrus incidence of female mice, increasing the number of estrus days in the cycles.

The estrous cycle is governed by the level of GnRH secretion from the hypothalamus, which stimulates the pituitary gland to release FSH and LH; these hormones regulate the ovarian cycle, resulting in the production of sex-steroid hormones (Smith, 2009). We measured the levels of GnRH, FSH, and LH in the plasma of female mice following 8 weeks of UVB or mock treatment and found a significant rise in these hormones following UVB treatment (Figure 3C). These data demonstrate that UVB treatment induces the production of hormones involved in the brain-gonadal axis.

FSH and LH regulate follicle growth in the ovaries, leading to ovulation (Smith, 2009). Therefore, we surgically resected the ovaries from UVB-treated and mock-treated control female mice in their proestrus/estrus stage to assess the effect of the UVB treatment on ovarian morphology. Interestingly, we found a significant increase in the size and weight of the ovaries of UVB-treated compared with mock-treated female mice (Fig-

ure 3D, left and middle panel), which was reflected in their histology (Figure 3D, right panel). Moreover, there was a significant increase in the expression of mRNAs encoding the progesterone receptor (PGR), androgen receptor (AR), and estrogen receptors (ESR1 and ESR2) in ovaries of UVB-treated females compared with control females (Figure 3E). We also observed significant upregulation in the enzymes involved in sex-steroid biosynthesis in UVB-treated females compared with control females (Figure S3B). AMH suppresses the cyclic recruitment of primordial follicles into the pool of growing follicles and inhibits FSH-dependent follicle recruitment (Dewailly et al., 2016), thus playing an important role in maintaining the ovarian reserve (Visser et al., 2006). AMH levels are an indicator of a female's ovarian reserve, and the number of oocytes with high AMH levels reflect a prolonged fertility window (Santoro, 2017). Upon UVB treatment, we found significant upregulation of the expression of AMH and AMHR2, which encode the AMH receptor, in the ovaries of female mice (Figure 3F), suggesting an increase in the pool of growing follicles. Altogether, our data indicate that UVB treatment of female mice enhances their estrous cycle, gonadotropin secretion, follicle growth, and sex-steroid synthesis.

p53 modulates UVB-mediated sexual behavior and ovarian changes

Skin interacts with solar/UVB light and has been suggested to result in production and release of hormones (Fell et al., 2014; Skobowiat and Slominski, 2015). Therefore, we reasoned that the skin plays a role in hormone-related social, sexual, and reproductive behavior in response to solar/UVB radiation. To identify the regulators that drive the sexual behavior and ovarian changes induced by UVB, we determined the overlap of the upstream transcription regulators upregulated in mouse plasma proteomes upon UVB treatment by Ingenuity pathway analysis (IPA) (Table S2), with the top 10 UVB-related transcription factors identified by GeneCards and the list of skin regulators involved in UVB response identified by GeneCards. The overlap of these three lists indicated that p53 is a potential regulator (Figure 4A; Table S3). Furthermore, p53 target genes, identified by IPA, are significantly enriched in biological processes involved in behavior and reproduction (Figure S4A), which is in line with
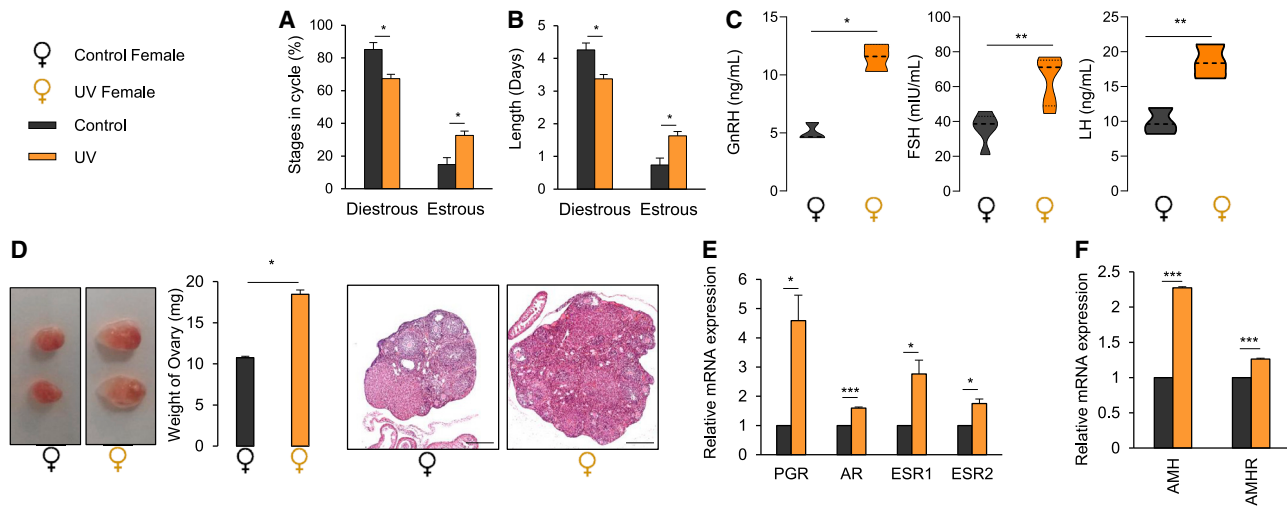
Figure 3. Daily UVB treatment increases estrus incidence and the number of growing follicles

(A) Percentage total of the proestrus/estrus stage (estrus) and metestrus/diestrus stage (diestrus) of the control or UVB-treated female estrous cycle.

(B) Length of the estrous cycle in a control or UVB-treated female.

(C) Plasma levels of GnRH (n = 3), FSH (n = 5), and LH (n = 3) of control or UVB-treated female mice.

(D) Representative photograph of the ovaries (left), the weight of ovaries in milligrams (middle), and representative H&E staining of female mice ovaries after 8 weeks of control or UVB treatment (right; scale bar, 500 μm).

(E) Relative mRNA expression from ovary section genes involved in female steroidogenesis after an 8-week control or UVB treatment.

(F) Relative expression of *AMH* and *AMHR* from an ovary section after an 8-week control or UVB treatment.

Data are presented as means ± SEM, n = 4 (A, B, E, and F), n = 3 (D). For data analysis, a two-tailed, unpaired Student's t test was performed. *p < 0.05; **p < 0.01; ***p < 0.001; ns, not statistically significant

our observations. Therefore, we hypothesized that the skin p53 modulates sexual behavior via a skin-brain-gonadal axis.

To test whether the UVB-induced sexual behavior changes we observed are p53 dependent, we crossed mice that express Cre specifically in keratinocytes (under the *K14* promotor) with *p53* floxed mice (Marino et al., 2000) to generate a conditional *p53* knockout in epidermal keratinocytes (p53^flox/flox K14-Cre^+/+), referred to here as p53-KO mice (Fell et al., 2014); wild-type p53 littermates (p53^flox/flox K14-Cre^−/−), referred to here as p53-WT, were used as controls (Figure S4B). We treated the p53-KO and p53-WT mice daily with UVB in a dose of 50 mJ/cm². There was a significant decrease in the levels of p53 in the whole skin of mice, as shown at protein level (Figure S4C) and at mRNA levels for *p53* and its downstream target *p21* in the skin (Figure S4D). These results validated the efficiency of the knockout of *p53* in epidermal keratinocytes. Consistent with the known role of p53 in the pigmentation response (Malcov-Brog et al., 2018), there was no increase in skin pigmentation in the p53-KO mice after 5 weeks of UVB treatment (Figure S4E). There were no differences in body weight between these mice before and after treatment (Figure S4F).

No increases in the circulating levels of GnRH, LH, or FSH were detected upon UVB treatment in the p53-KO females (Figure 4B). Moreover, no changes in ovary size, weight, or histology were noted in UVB-treated p53-KO females compared with mock-treated p53-KO females (Figure 4C). Furthermore, there were no differences in the levels of mRNAs encoding steroidogenic hormone receptors (*PGR*, *AR*, *ESR1*, and *ESR2*) (Figure 4D), in the expression level of the enzymes related to each of these receptors in the ovaries (Figure S4G) or in the expression

of *AMH* and *AMHR* (Figure 4E) when UVB-treated and mock-treated control p53-KO females were compared. These data support our hypothesis that skin p53 drives the changes in the ovaries and mediates sex-steroid induction upon UVB treatment.

To evaluate how skin p53 influences sexual behavior, UVB-treated and mock-treated control p53-WT and p53-KO mice were subjected to the mating test (Figure 1B). All females were in the estrus/proestrus stage. We found no difference in the anogenital sniffing behavior of p53-WT and p53-KO males toward UVB-treated or mock-treated p53-WT females (Figure 4F, left panel). In contrast, the amount of sniffing toward the UVB-treated p53-KO females was significantly reduced compared with that toward the mock-treated p53-KO females and UVB-treated p53-WT females (Figure 4F, left panel). Furthermore, we found a significant increase in the sniffing behavior of females (both p53-WT and p53-KO) toward UVB-treated p53-WT males compared with mock-treated control p53-WT males, but no enhancement of sniffing behavior was observed toward the UVB-treated p53-KO males (Figure 4F, right panel). This suggests that UVB treatment induces a male mouse odor cue that depends on skin p53.

Both p53-WT and p53-KO males exhibited significant enhancement of facial and genital grooming in the presence of a UVB-treated p53-WT female compared with a control p53-WT female, whereas this UVB effect did not occur in the presence of the p53-KO females (Figure 4G, left panel). Furthermore, we noted an increase in the grooming behavior of females (both p53-WT and p53-KO) in the presence of UVB-treated p53-WT males compared with control p53-WT males, a feature not
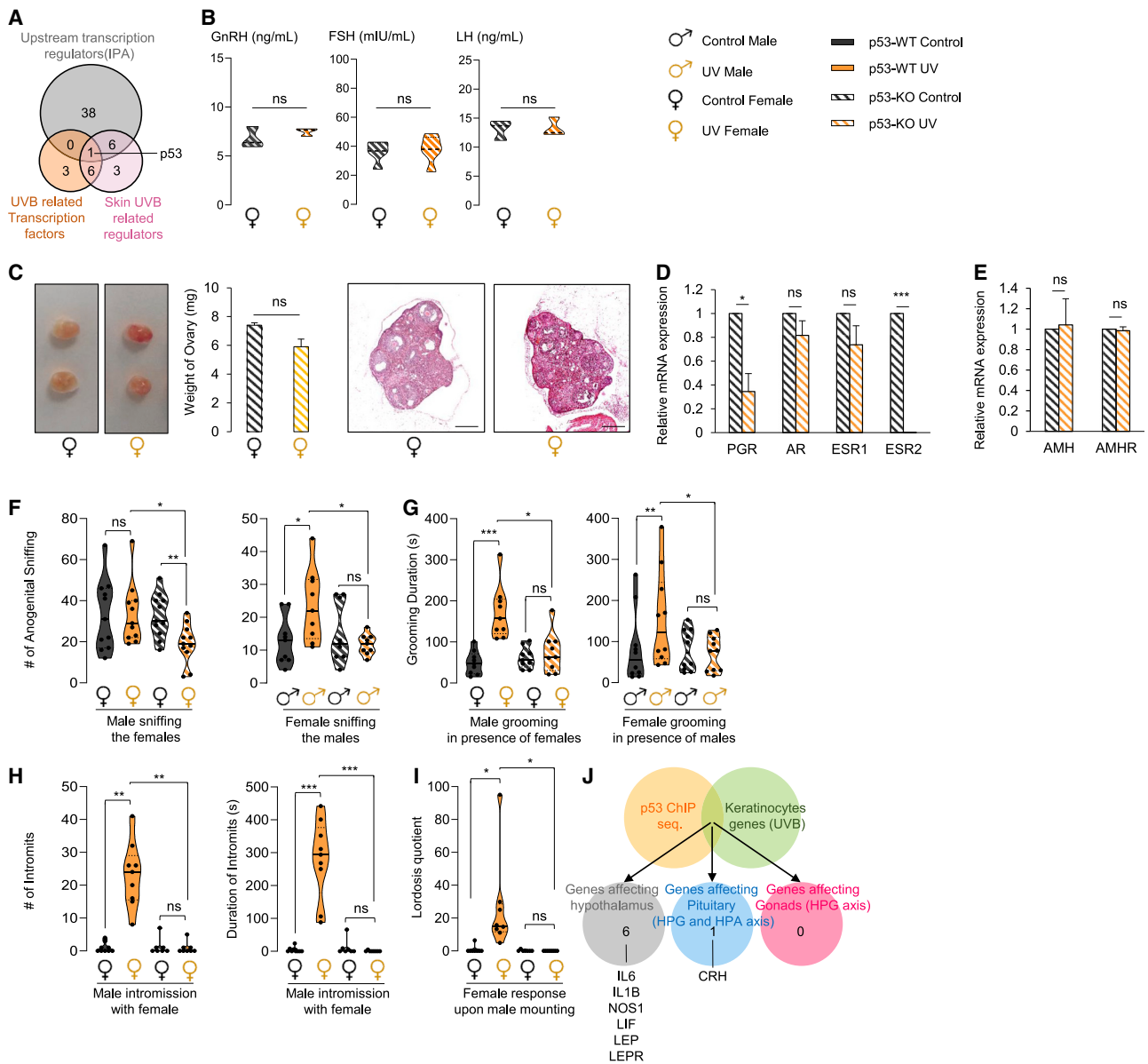
Figure 4. p53 modulates UVB treatment-mediated sexual behavior and ovarian changes

(A) Overlap of predicted upstream regulators from mouse upon UVB treatment of 8 weeks with the top 10 UVB-related transcription factors (GeneCards) and with skin regulators involved in UVB response (GeneCards).

(B) Plasma levels of GnRH (n = 3), FSH (n = 5), and LH (n = 3) in p53-KO females.

(C) Photograph of representative ovaries (left), weight in milligrams (mg) of ovaries (middle), and representative H&E staining (right; scale bar, 500 μm) from p53-KO females ovaries.

(D) Relative mRNA expression levels of genes involved in steroidogenesis from p53-KO female ovaries.

(E) Relative mRNA expression levels of *AMH* and *AMHR* from p53-KO female ovaries.

(F) Total number of anogenital sniffing events by males (control- or UVB-treated p53-WT and p53-KO) toward control- or UVB-treated p53-WT or p53-KO females (left). Total number of anogenital sniffing events by females (control- or UVB-treated p53-WT and p53-KO) toward control- or UVB-treated p53-WT or p53-KO males (right).

(G) Total time spent self-grooming by males (control- or UVB-treated p53-WT and p53-KO) in the presence of control- or UVB-treated p53-WT or p53-KO females (left panel). Total time spent self-grooming by females (control- or UVB-treated p53-WT and p53-KO) in the presence of control- or UVB-treated p53-WT or p53-KO males (right panel).

(H) Total number of intromissions (left) and total duration of intromissions (right) by males (control- or UVB-treated p53-WT and p53-KO) with control- or UVB-treated p53-WT or p53-KO females.

(I) UVB- or control-treated p53-WT or p53-KO females' lordosis quotient with control- and UVB-treated p53-WT or p53-KO males.

observed in the presence of p53-KO males (Figure 4G, right panel). The total number and duration of successful intromissions by males (both p53-WT and p53-KO) on UVB-treated p53-WT females were significantly higher than on control p53-WT females, whereas no change was observed toward p53-KO females (Figure 4H).

The lordotic response of a female was significantly higher in UVB-treated p53-WT mice than in mock-treated control p53-WT mice; there was no difference in p53-KO females (Figure 4I). We also found that UVB-treated p53-WT males have significantly higher levels of testosterone in their plasma than do mock-treated p53-WT males and that this UVB effect was abolished in p53-KO males (Figure S4H, left panel). No change was observed in female testosterone levels upon UVB treatment (Figure S4H, right panel). These observations support our finding that testosterone appears to be influenced by UVB-induced skin p53. These data indicate that the enhancement of female and male attractiveness to the opposite sex induced by UVB treatment depends on p53 in the skin.

To further explore the mechanism by which p53 controls sexual behavior upon UVB treatment, we overlapped two datasets, p53 binding genes (identified using chromatin immunoprecipitation sequencing [ChIP-seq]) (Nguyen et al., 2018) and UVB-affected keratinocyte genes (identified using GeneCards) (Figure 4J). To identify the downstream targets of p53 (i.e., UVB-induced keratinocyte genes bound by p53), we overlapped these genes with genes known to affect the hypothalamus (Kang et al., 2000; McCann et al., 2003; Ray et al., 1996; Schmidt et al., 1995; Slominski et al., 2012), genes known to affect the pituitary hypothalamus-pituitary-gonadal (HPG) and HPA axes (Rawindraraj et al., 2019), or genes known to affect the gonadal HPG axis (Figure 4J). We found six overlapping genes that affect the hypothalamus: *IL6*, *LIF*, *IL-1β*, *NOS*, *Leptin*, and *LEP-R* (Figure 4J; Table S4). IL-6 and LIF are known to increase the expression of POMC to enhance LH, FSH, and ACTH effects on the downstream gonads and adrenal gland (Chida et al., 2005; Ray et al., 1996). Interleukin (IL)-1β increases the expression of CRH and GnRH from the hypothalamus (Kang et al., 2000; Schmidt et al., 1995). NOS increases luteinizing hormone releasing hormone (LHRH) levels (McCann et al., 2003), and vice versa (Garrel et al., 1998). LHRH controls female lordosis and male sexual behavior (McCann et al., 2003). Moreover, we found one overlapping gene, *CRH*, that affects the pituitary. The CRH protein is released from the skin upon UVB treatment and acts on the local and central HPA axis (Skobowiat and Slominski, 2015; Skobowiat et al., 2011).

We observed significant upregulation of *IL1B*, *CRH*, and *IL6* expression in UVB-treated p53-WT males, whereas the expression of these genes remained unchanged in the UVB-treated p53-KO males (Figure S4I, upper panel). Furthermore, we observed significant upregulation of *IL1B*, *IL6*, *LIF*, and *CRH*, as expected based on previous work (Skobowiat and Slominski, 2015), and of *NOS1* in UVB-treated p53-WT females, but not in

UVB-treated p53-KO females, compared with mock-treated controls (Figure S4I, lower panel). Altogether, these findings demonstrate that p53 expressed in epidermal keratinocytes regulates sexual behavior and ovarian changes through a skin-brain-gonadal axis.

Solar exposure enhances human sex-related steroids

To examine the relevance of mouse data to humans, we recruited volunteers (n = 9 men, n = 10 women; age 18–55 years) who were asked to avoid sun exposure for 2 days and then spend approximately 25 min in the sun on a bright sunny midday; this resulted in a dose of approximately 2,000 mJ/cm^2 UV radiation (measured using a UVX radiometer). Blood samples were collected on the day before sun exposure and approximately the same time on the day of sun exposure. Similar to the mouse proteome data (Figure 1A), we found a significant positive activation Z score for upstream regulators β-estradiol, progesterone, testosterone, and estrogen in men (Figure 5A, left panel) and for estrogen, progesterone, and testosterone in women following solar exposure compared with the control day before exposure (Figure 5A, right panel).

Furthermore, we analyzed the testosterone levels of men aged 21–25 years (n = 13,086) from the Maccabi Health Service (Chodick et al., 2020) and observed a significant peak in total testosterone level during the summer (July), indicative of testosterone seasonal variation (Figure 5B). This is in line with a previous report that testosterone levels increase in men following UV radiation (Myerson and Neustadt, 1939). Finally, to determine how pigment phenotype affects these solar responses, we retrieved testosterone-level data of men aged 20–50 years from the Clalit Health Services data-sharing platform (Israel) and divided them into two groups based on the amount of ultraviolet radiation (UVR) in their country of origin. Testosterone levels were significantly higher (n = 1,607, p = 0.004) in men originating from countries with low UVR (UV < 2,500 J/m^2) compared with individuals who originated from countries with high UVR (UV ≥ 4,500 J/m^2) during summer months (May–September) for all body mass index values (Figure S5, left panel). No significant differences (n = 2,309, p = 0.499) were observed during the winter months (October–April) (Figure S5, right panel). Because skin coloration is strongly related to levels of UVR in a given country (Chaplin, 2004), our data support the involvement of the skin reaction to UVR in regulation of sexual behavior. Altogether, our data suggest enhancement of sex steroids upon solar exposure and demonstrate a positive correlation between solar exposure and testosterone levels in human males.

DISCUSSION

Fitness is defined by the individual's reproductive success (Zimmer et al., 2016). Conception must be timed so that offspring are born when they have the highest chances of survival and reproduction. This is likely the reason for seasonality in birth rates in

---

(J) Overlap between p53 DNA binding-based ChIP-seq (Nguyen et al., 2018), UVB-affected keratinocyte genes (GeneCards), and genes affecting hypothalamic, pituitary, and gonad expression (Kang et al., 2000; McCann et al., 2003; Ray et al., 1996; Schmidt et al., 1995; Slominski et al., 2012).
Data are presented as means ± SEM, n = 4 (C–E), n = 3 (F–I). For data analysis, a two-tailed, unpaired Student's t test (B–E) or two-way ANOVA (F–I) was performed. *p < 0.05; **p < 0.01; ***p < 0.001; ns, not statistically significant.
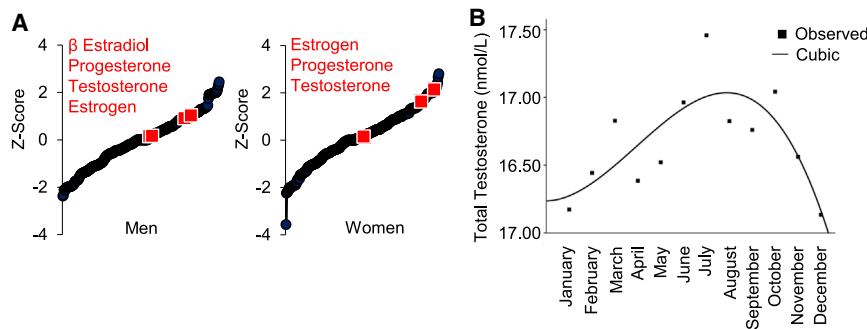
Figure 5. Solar exposure enhances human sex-related steroids

(A) Predicted upstream regulators of the differential blood plasma proteins from humans following a single solar exposure (2,000 mJ/cm^2 UV) (n = 5 humans for each condition).

(B) Total testosterone levels of men aged 21–25 years (n = 13,086). Plot depicts monthly means on a cubic spline of calendar month (January–December; 2 degrees of freedom).

humans. There is a unimodal spring-summer (end of April–May) peak in conceptions in most of Europe and a strongly bimodal distribution in North America, with peaks in spring and autumn (Roenneberg, 2004). Photoperiod and temperature have been suggested to be the major environmental factors affecting this seasonality (Roenneberg and Aschoff, 1990a, 1990b). Because we showed a direct response to UVB, the source is not the endogenous circannual clock, which generates seasonal changes in physiology and behavior in the absence of environmental cues (Scanes, 2015). Therefore, UVB may serve as a backup mechanism, ensuring optimal reproduction timing and direct influence on fitness. It is interesting that industrialization, which shifted work from outdoors to indoors with eternal summer conditions, characterized by a long photoperiod and mild temperatures with almost no seasonality (Stevenson et al., 2015), happened in parallel to an amplitude reduction in peaks in human conceptions observed in today's industrialized nations (Foster and Roenneberg, 2008; Roenneberg, 2004). It is possible that the reduced exposure to UVB contributed to this change.

Our data suggest skin-brain crosstalk, in which the skin acts as a dermato-endocrine organ, releasing hormones that affect the hypothalamus-pituitary-gonadal axis. The mechanism of action may be similar to that of β-endorphins (Fell et al., 2014) and CRH (Skobowiat and Slominski, 2015), which are released from the skin and affect the opioid system and axis, respectively, and/or to nerve fibers, the immune system, or as-yet-unknown regulators. Because eyes of mice and of human volunteers were not covered, we cannot exclude the possibility that solar/UV radiation to the eye affected the observed sexual behavior. UVB exposure via the eye activates the hypothalamopituitary proopiomelanocortin system, which is upstream of the HPA and HPG axes (Hiramoto et al., 2003). However, when we depleted p53 from skin keratinocytes, we observed suppression of the UVB-induced sexual behavior traits, as well as a significant decrease in the hormones of the HPG axis, which favor our hypothesis that in addition to the eyes, the skin has an active part in regulating sexuality.

Vitamin D synthesis is affected by UV absorption, which depends on the skin tone of the individual (Webb et al., 2018; Richard et al., 2017); thus, individuals with the Fitzpatrick V (FST V) skin type must receive a greater UV dose per unit time to synthesize vitamin D compared with individuals with lighter skin (Webb et al., 2018). In addition to the seasonality of birth rates, conception rates, ovulation, socioeconomic status, and age group as fertility effectors (Bobak and Gjonca, 2001; Lam

et al., 1994; Stolwijk et al., 1996), we propose that pigment phenotype might play a role in regulating the skin-brain-gonadal axis, thereby regulating sexual behavior.

All skin layers are innervated by sensory, sympathetic, and parasympathetic nerve fibers that relay signals to the brain and receive cues from it (Slominski et al., 2012). Sensory signals from the skin to the brain include temperature, touch, pain, stretch, itch, and vibration; they are sensed by skin receptors that transfer the stimuli via nerve fibers directly to the brain (Roosterman et al., 2006). Signals from the brain to the skin include thermoregulation, sweat-gland function, blood flow, adnexal functions (Roosterman et al., 2006), and hair graying (Zhang et al., 2020).

Another mode of skin-brain crosstalk involves the combined neural signals from the preoptic hypothalamus and peripheral nerves that together trigger eccrine sweat glands (Stowers and Liberles, 2016). In a response that is sex dependent (Stowers and Liberles, 2016), pheromones are mainly secreted in axillary sweat, which contains the odorous 16-androstenes (Verhaeghe et al., 2013). Axillary secretions originate from apocrine odor glands, eccrine sweat glands, and sebaceous glands located in the skin (Verhaeghe et al., 2013). Pheromones are inducers of communication and behavioral responses, including sexuality and mating (Ferrero et al., 2013; Roberts et al., 2010; Stowers and Liberles, 2016; Verhaeghe et al., 2013). Although the neural triggers for pheromone synthesis and secretion are poorly understood, it has been established that eccrine sweat glands are controlled by hypothalamus cues (Stowers and Liberles, 2016). Therefore, we cannot exclude the possibility that part of the observed effect is mediated by pheromones: UVB radiation may alter hypothalamus activity or directly affect axillary secretion. Both possibilities should be further investigated. In line with this, knock down of p53 has been shown to trigger the DNA damage response in skin keratinocytes that results in peeling of these cells (Farmer et al., 1992; Fields and Jang, 1990; Levine et al., 2006; de Pedro et al., 2018). This by itself might be a trigger of attractiveness and should be investigated in the future.

It is worth putting in mind that species differences play an essential role in activating mating behavior via the circulating sex steroids. For example, female rhesus monkeys continue to mate with males for weeks after ovariectomy, wherein there is withdrawal of estradiol (Baum et al., 1977). In contrast, ovariectomized female mice cease to mate within few days of the

procedure and resume it only upon receiving an injection of estradiol benzoate followed by progesterone (Edwards, 1971). Likewise, male rhesus monkeys typically continue mating for many months after castration (Phoenix et al., 1973), whereas most strains of male mice stop mating within 3–4 weeks after castration (Thompson et al., 1976).

Our quantitative questionnaire results show that both sexes have a tendency toward higher levels of passion following UV treatment. Passion takes two forms, emotional and sexual. UVB radiation affected different components of passion in men than in women. UVB-treated women scored higher on questions about physical arousal that related more to sexual passion and idealizing the connection, whereas men scored higher on the cognitive dimension of passion, which involves obsessive thoughts about the partner and wanting to know more about her. The questionnaire we used measured romantic passion, rather than physiological/sexual passion, due to institutional review board (IRB) ethical concerns regarding sensitive sexually oriented questions. Future studies on this topic should address physiological arousal more directly and should be geared toward the precise identification of the different effects of UVB on the sexual behavior of men and women.

STAR★METHODS

Detailed methods are provided in the online version of this paper and include the following:

- KEY RESOURCES TABLE
- RESOURCE AVAILABILITY
  - ○ Lead contact
  - ○ Materials availability
  - ○ Data and code availability
- EXPERIMENTAL MODEL AND SUBJECT DETAILS
  - ○ Mouse models and habituation
  - ○ Human cohort
  - ○ Human cohort testosterone study
  - ○ Human questionnaire
- METHOD DETAILS
  - ○ UV treatment
  - ○ Melanin intensity quantification
  - ○ Mouse blood draw
  - ○ Human cohort Solar-exposure study
  - ○ Human blood draw
  - ○ Proteolysis and mass spectrometry
  - ○ Proteomic analysis
  - ○ ELISA
  - ○ Mating test
  - ○ Ultrasonic vocalization
  - ○ Elevated plus maze test
  - ○ Three-chamber test
  - ○ Male subject and two female stimuli
  - ○ Female subject and two male stimuli
  - ○ Female subject and two female stimuli
  - ○ Female subject, a male stimulus, and a novel-object stimulus
  - ○ Vaginal smears for estrous cycle evaluation
  - ○ RNA purification and qRT-PCT
- Histology
- Genotyping
- Immunoblotting
- QUANTIFICATION AND STATISTICAL ANALYSIS

REFERENCES

Achiraman, S., SankarGanesh, D., Kannan, S., Kamalakkannan, S., Nirmala, N., and Archunan, G. (2014). Response of male mice to odours of female mice in different stages of oestrous cycle: self-grooming behaviour and the effect of castration. Indian J. Exp. Biol. 52, 30–35.

Ajayi, A.F., and Akhigbe, R.E. (2020). Staging of the estrous cycle and induction of estrus in experimental rodents: an update. Fertil. Res. Pract. 6, 5.

Asaba, A., Hattori, T., Mogi, K., and Kikusui, T. (2014). Sexual attractiveness of male chemicals and vocalizations in mice. Front. Neurosci. 8, 231.

Cell Reports
Article

Bae, J.M., Jung, H.M., Hong, B.Y., Lee, J.H., Choi, W.J., Lee, J.H., and Kim, G.M. (2017). Phototherapy for vitiligo: A systematic review and meta-analysis. JAMA Dermatol. *153*, 666–674.

Barbieri, R.L. (2014). The endocrinology of the menstrual cycle. Methods Mol. Biol. *1154*, 145–169.

Baum, M.J., Everitt, B.J., Herbert, J., and Keverne, E.B. (1977). Hormonal basis of proceptivity and receptivity in female primates. Arch. Sex. Behav. *6*, 173–192.

Beach, F.A. (1976). Sexual attractivity, proceptivity, and receptivity in female mammals. Horm. Behav. *7*, 105–138.

Bobak, M., and Gjonca, A. (2001). The seasonality of live birth is strongly influenced by socio-demographic factors. Hum. Reprod. *16*, 1512–1517.

Buss, A.H., and Perry, M. (1992). The aggression questionnaire. J. Pers. Soc. Psychol. *63*, 452–459.

Caligioni, C.S. (2009). Assessing reproductive status/stages in mice. Curr. Protoc. Neurosci. *4* (*Appendix*), 4I.

Cameron, H., Dawe, R.S., Yule, S., Murphy, J., Ibbotson, S.H., and Ferguson, J. (2002). A randomized, observer-blinded trial of twice vs. three times weekly narrowband ultraviolet B phototherapy for chronic plaque psoriasis. Br. J. Dermatol. *147*, 973–978.

Chaplin, G. (2004). Geographic distribution of environmental factors influencing human skin coloration. Am. J. Phys. Anthropol. *125*, 292–302.

Chida, D., Imaki, T., Suda, T., and Iwakura, Y. (2005). Involvement of corticotropin-releasing hormone- and interleukin (IL)-6-dependent proopiomelanocortin induction in the anterior pituitary during hypothalamic-pituitary-adrenal axis activation by IL-1α. Endocrinology *146*, 5496–5502.

Chodick, G., Epstein, S., and Shalev, V. (2020). Secular trends in testosterone—findings from a large state-mandate care provider. Reprod. Biol. Endocrinol. *18*, 19.

Clarke, S., and Trowill, J.A. (1971). Sniffing and motivated behavior in the rat. Physiol. Behav. *6*, 49–52.

Costantini, F., and D'Amato, F. (2006). Ultrasonic vocalizations in mice and rats: social contexts and functions. Dong Wu Xue Bao *52*, 619–633.

Cox, J., and Mann, M. (2008). MaxQuant enables high peptide identification rates, individualized p.p.b.-range mass accuracies and proteome-wide protein quantification. Nat. Biotechnol. *26*, 1367–1372.

de Pedro, I., Alonso-Lecue, P., Sanz-Gómez, N., Freije, A., and Gandarillas, A. (2018). Sublethal UV irradiation induces squamous differentiation via a p53-independent, DNA damage-mitosis checkpoint. Cell Death Dis. *9*, 1094.

Dewailly, D., Robin, G., Peigne, M., Decanter, C., Pigny, P., and Catteau-Jonard, S. (2016). Interactions between androgens, FSH, anti-Müllerian hormone and estradiol during folliculogenesis in the human normal and polycystic ovary. Hum. Reprod. Update *22*, 709–724.

Dror, S., Sander, L., Schwartz, H., Sheinboim, D., Barzilai, A., Dishon, Y., Apcher, S., Golan, T., Greenberger, S., Barshack, I., et al. (2016). Melanoma miRNA trafficking controls tumour primary niche formation. Nat. Cell Biol. *18*, 1006–1017.

Edwards, D.A. (1971). Neonatal administration of androstenedione, testosterone or testosterone propionate: effects on ovulation, sexual receptivity and aggressive behavior in female mice. Physiol. Behav. *6*, 223–228.

Farmer, G., Bargonetti, J., Zhu, H., Friedman, P., Prywes, R., and Prives, C. (1992). Wild-type p53 activates transcription *in vitro*. Nature *358*, 83–86.

Fell, G.L., Robinson, K.C., Mao, J., Woolf, C.J., and Fisher, D.E. (2014). Skin β-endorphin mediates addiction to UV light. Cell *157*, 1527–1534.

Ferrero, D.M., Moeller, L.M., Osakada, T., Horio, N., Li, Q., Roy, D.S., Cichy, A., Spehr, M., Touhara, K., and Liberles, S.D. (2013). A juvenile mouse pheromone inhibits sexual behaviour through the vomeronasal system. Nature *502*, 368–371.

Fields, S., and Jang, S.K. (1990). Presence of a potent transcription activating sequence in the p53 protein. Science *249*, 1046–1049.

Foster, R.G., and Roenneberg, T. (2008). Human responses to the geophysical daily, annual and lunar cycles. Curr. Biol. *18*, R784–R794.

Garrel, G., Lerrant, Y., Siriostis, C., Bérault, A., Magre, S., Bouchaud, C., and Counis, R. (1998). Evidence that gonadotropin-releasing hormone stimulates gene expression and levels of active nitric oxide synthase type I in pituitary gonadotrophs, a process altered by desensitization and, indirectly, by gonadal steroids. Endocrinology *139*, 2163–2170.

Glaich, O., Parikh, S., Bell, R.E., Mekahel, K., Donyo, M., Leader, Y., Shayevitch, R., Sheinboim, D., Yannai, S., Hollander, D., et al. (2019). DNA methylation directs microRNA biogenesis in mammalian cells. Nat. Commun. *10*, 5657.

Golan, T., Messer, A.R., Amitai-Lange, A., Melamed, Z., Ohana, R., Bell, R.E., Kapitansky, O., Lerman, G., Greenberger, S., Khaled, M., et al. (2015). Interactions of Melanoma Cells with Distal Keratinocytes Trigger Metastasis via Notch Signaling Inhibition of MITF. Mol. Cell *59*, 664–676.

Haga, S., Hattori, T., Sato, T., Sato, K., Matsuda, S., Kobayakawa, R., Sakano, H., Yoshihara, Y., Kikusui, T., and Touhara, K. (2010). The male mouse pheromone ESP1 enhances female sexual receptive behaviour through a specific vomeronasal receptor. Nature *466*, 118–122.

Hatfield, E., and Sprecher, S. (1986). Measuring passionate love in intimate relationships. J. Adolesc. *9*, 383–410.

Hiramoto, K., Yanagihara, N., Sato, E.F., and Inoue, M. (2003). Ultraviolet B irradiation of the eye activates a nitric oxide-dependent hypothalamopituitary proopiomelanocortin pathway and modulates functions of α-melanocyte-stimulating hormone-responsive cells. J. Invest. Dermatol. *120*, 123–127.

Hölzle, E., and Hönigsmann, H. (2005). [UV-radiation—sources, wavelength, environment]. J. Dtsch. Dermatol. Ges. *3* (*Suppl 2*), S3–S10.

Jones, E.K.M., Prescott, N.B., Cook, P., White, R.P., and Wathes, C.M. (2001). Ultraviolet light and mating behaviour in domestic broiler breeders. Br. Poult. Sci. *42*, 23–32.

Kalueff, A.V., Stewart, A.M., Song, C., Berridge, K.C., Graybiel, A.M., and Fentress, J.C. (2016). Neurobiology of rodent self-grooming and its value for translational neuroscience. Nat. Rev. Neurosci. *17*, 45–59.

Kang, S.S., Kim, S.R., Leonhardt, S., Jarry, H., Wuttke, W., and Kim, K. (2000). Effect of interleukin-1β on gonadotropin-releasing hormone (GnRH) and GnRH receptor gene expression in castrated male rats. J. Neuroendocrinol. *12*, 421–429.

Kerchner, M. (2004). Ultrasonic courtship vocalizations of adult male mice: A laboratory exercise illustrating comparable activation by either estradiol or testosterone. J. Undergrad. Neurosci. Educ. *2*, A50–A61.

Kim, H., Son, J., Yoo, H., Kim, H., Oh, J., Han, D., Hwang, Y., and Kaang, B.K. (2016). Effects of the female Estrous cycle on the sexual behaviors and ultrasonic vocalizations of male C57BL/6 and autistic BTBR T+ tf/J Mice. Exp. Neurobiol. *25*, 156–162.

Kimchi, T., Xu, J., and Dulac, C. (2007). A functional circuit underlying male sexual behaviour in the female mouse brain. Nature *448*, 1009–1014.

Kuukasjärvi, S., Eriksson, C.J.P., Koskela, E., Mappes, T., Nissinen, K., and Rantala, M.J. (2004). Attractiveness of women's body odors over the menstrual cycle: The role of oral contraceptives and receiver sex. Behav. Ecol. *15*, 579–584.

Lam, D.A., Miron, J.A., and Riley, A. (1994). Modeling seasonality in fecundability, conceptions, and births. Demography *31*, 321–346.

Levine, A.J., Hu, W., and Feng, Z. (2006). The P53 pathway: what questions remain to be explored? Cell Death Differ. *13*, 1027–1036.

Malcov-Brog, H., Alpert, A., Golan, T., Parikh, S., Nordlinger, A., Netti, F., Sheinboim, D., Dror, I., Thomas, L., Cosson, C., et al. (2018). UV-Protection Timer Controls Linkage between Stress and Pigmentation Skin Protection Systems. Mol. Cell *72*, 444–456.e7.

Marino, S., Vooijs, M., van Der Gulden, H., Jonkers, J., and Berns, A. (2000). Induction of medulloblastomas in p53-null mutant mice by somatic inactivation of Rb in the external granular layer cells of the cerebellum. Genes Dev. *14*, 994–1004.

McCann, S., Mastronardi, C., Walczewska, A., Karanth, S., Rettori, V., and Yu, W. (2003). The Role of Nitric Oxide (NO) in Control of LHRH Release that

Mediates Gonadotropin Release and Sexual Behavior. Curr. Pharm. Des. *9*, 381–390.

Mitchell, D.L., Fernandez, A.A., Garcia, R., Paniker, L., Lin, K., Hanninen, A., Zigelsky, K., May, M., Nuttall, M., Lo, H.H., et al. (2014). Acute exposure to ultraviolet-B radiation modulates sex steroid hormones and receptor expression in the skin and may contribute to the sex bias of melanoma in a fish model. Pigment Cell Melanoma Res. *27*, 408–417.

Mitra, R., and Sapolsky, R.M. (2012). Short-term enrichment makes male rats more attractive, more defensive and alters hypothalamic neurons. PLoS ONE *7*, e36092.

Muller, M.N. (2017). Testosterone and reproductive effort in male primates. Horm. Behav. *91*, 36–51.

Myerson, A., and Neustadt, R. (1939). Influence of ultraviolet irradiation upon excretion of sex hormones in the male. Endocrinology 25, 7–12.

Nghiem, D.X., Kazimi, N., Mitchell, D.L., Vink, A.A., Ananthaswamy, H.N., Kripke, M.L., and Ullrich, S.E. (2002). Mechanisms underlying the suppression of established immune responses by ultraviolet radiation. J. Invest. Dermatol. *119*, 600–608.

Nguyen, T.T., Grimm, S.A., Bushel, P.R., Li, J., Li, Y., Bennett, B.D., Lavender, C.A., Ward, J.M., Fargo, D.C., Anderson, C.W., et al. (2018). Revealing a human p53 universe. Nucleic Acids Res. *46*, 8153–8167.

Perez-Riverol, Y., Csordas, A., Bai, J., Bernal-Llinares, M., Hewapathirana, S., Kundu, D.J., Inuganti, A., Griss, J., Mayer, G., Eisenacher, M., et al. (2019). The PRIDE database and related tools and resources in 2019: Improving support for quantification data. Nucleic Acids Res. *47*, D442–D450.

Phoenix, C.H., Goy, R.W., Gerall, A.A., and Young, W.C. (1959). Organizing action of prenatally administered testosterone propionate on the tissues mediating mating behavior in the female guinea pig. Endocrinology *65*, 369–382.

Phoenix, C.H., Slob, A.K., and Goy, R.W. (1973). Effects of castration and replacement therapy on sexual behavior of adult male rhesuses. J. Comp. Physiol. Psychol. *84*, 472–481.

Pradhan, A., and Olsson, P.E. (2015). Zebrafish sexual behavior: role of sex steroid hormones and prostaglandins. Behav. Brain Funct. *11*, 23.

Puts, D.A. (2010). Beauty and the beast: Mechanisms of sexual selection in humans. Evol. Hum. Behav. *31*, 157–175.

Rawindraraj, A.D., Basit, H., and Jialal, I. (2019). Physiology, Anterior Pituitary (StatPearls).

Ray, D.W., Ren, S.G., and Melmed, S. (1996). Leukemia inhibitory factor (LIF) stimulates proopiomelanocortin (POMC) expression in a corticotroph cell line. Role of STAT pathway. J. Clin. Invest. *97*, 1852–1859.

Richard, A., Rohrmann, S., and Quack Lötscher, K.C. (2017). Prevalence of vitamin D deficiency and its associations with skin color in pregnant women in the first trimester in a sample from Switzerland. Nutrients *9*, E260.

Roberts, S.C., Havlicek, J., Flegr, J., Hruskova, M., Little, A.C., Jones, B.C., Perrett, D.I., and Petrie, M. (2004). Female facial attractiveness increases during the fertile phase of the menstrual cycle. Proc. Biol. Sci. *271* (*Suppl 5*), S270–S272.

Roberts, S.A., Simpson, D.M., Armstrong, S.D., Davidson, A.J., Robertson, D.H., McLean, L., Beynon, R.J., and Hurst, J.L. (2010). Darcin: a male pheromone that stimulates female memory and sexual attraction to an individual male's odour. BMC Biol. *8*, 75.

Roenneberg, T., and Aschoff, J. (1990a). Annual rhythm of human reproduction: I. Biology, sociology, or both? J. Biol. Rhythms *5*, 195–216.

Roenneberg, T., and Aschoff, J. (1990b). Annual Rhythm of Human Reproduction: II. Environmental Correlations. J. Biol. Rhythms *5*, 217–239.

Roenneberg, T. (2004). The decline in human seasonality. J. Biol. Rhythms *19*, 193–195, discussion 196–197.

Roosterman, D., Goerge, T., Schneider, S.W., Bunnett, N.W., and Steinhoff, M. (2006). Neuronal control of skin function: the skin as a neuroimmunoendocrine organ. Physiol. Rev. *86*, 1309–1379.

Rosner, J., and Sarao, M.S. (2019). Physiology, Female Reproduction (StatPearls).

Santoro, N. (2017). Using Antimüllerian Hormone to Predict Fertility. JAMA *318*, 1333–1334.

C.G. Scanes, ed. (2015). Sturkie's Avian Physiology, Sixth Edition (Academic Press).

Schellino, R., Trova, S., Cimino, I., Farinetti, A., Jongbloets, B.C., Pasterkamp, R.J., Panzica, G., Giacobini, P., De Marchis, S., and Peretto, P. (2016). Opposite-sex attraction in male mice requires testosterone-dependent regulation of adult olfactory bulb neurogenesis. Sci. Rep. *6*, 36063.

Schmidt, E.D., Janszen, A.W., Wouterlood, F.G., and Tilders, F.J. (1995). Interleukin-1-induced long-lasting changes in hypothalamic corticotropin-releasing hormone (CRH)—neurons and hyperresponsiveness of the hypothalamus-pituitary-adrenal axis. J. Neurosci. *15*, 7417–7426.

Skobowiat, C., and Slominski, A.T. (2015). UVB Activates Hypothalamic-Pituitary-Adrenal Axis in C57BL/6 Mice. J. Invest. Dermatol. *135*, 1638–1648.

Skobowiat, C., Dowdy, J.C., Sayre, R.M., Tuckey, R.C., and Slominski, A. (2011). Cutaneous hypothalamic-pituitary-adrenal axis homolog: regulation by ultraviolet radiation. Am. J. Physiol. Endocrinol. Metab. *301*, E484–E493.

Skobowiat, C., Postlethwaite, A.E., and Slominski, A.T. (2017). Skin Exposure to Ultraviolet B Rapidly Activates Systemic Neuroendocrine and Immunosuppressive Responses. Photochem. Photobiol. *93*, 1008–1015.

Slominski, A., and Wortsman, J. (2000). Neuroendocrinology of the skin. Endocr. Rev. *21*, 457–487.

Slominski, A.T., Zmijewski, M.A., Skobowiat, C., Zbytek, B., Slominski, R.M., and Steketee, J.D. (2012). Sensing the environment: regulation of local and global homeostasis by the skin's neuroendocrine system. Adv. Anat. Embryol. Cell Biol. *212* (*v, vii*), 1–115.

Slominski, A.T., Zmijewski, M.A., Zbytek, B., Tobin, D.J., Theoharides, T.C., and Rivier, J. (2013). Key role of CRF in the skin stress response system. Endocr. Rev. *34*, 827–884.

Slominski, A.T., Manna, P.R., and Tuckey, R.C. (2015). On the role of skin in the regulation of local and systemic steroidogenic activities. Steroids *103*, 72–88.

Slominski, A.T., Zmijewski, M.A., Plonka, P.M., Szaflarski, J.P., and Paus, R. (2018). How UV Light Touches the Brain and Endocrine System Through Skin, and Why. Endocrinology *159*, 1992–2007.

Smith, M.S. (2009). Estrus and menstrual cycles: Neuroendocrine control. In Encyclopedia of Neuroscience, L.R. Squire, ed. (Elsevier), pp. 1–5.

Stevenson, T.J., Visser, M.E., Arnold, W., Barrett, P., Biello, S., Dawson, A., Denlinger, D.L., Dominoni, D., Ebling, F.J., Elton, S., et al. (2015). Disrupted seasonal biology impacts health, food security and ecosystems. Proc. Biol. Sci. *282*, 20151453.

Stolwijk, A.M., Olsen, J., Schaumburg, I., Jongbloet, P.H., and Zielhuis, G.A. (1996). Seasonal variation in the time to pregnancy: a secondary analysis of three Danish databases. Eur. J. Epidemiol. *12*, 437–441.

Stowers, L., and Liberles, S.D. (2016). State-dependent responses to sex pheromones in mouse. Curr. Opin. Neurobiol. *38*, 74–79.

Svobodová, A.R., Galandáková, A., Sianská, J., Doležal, D., Lichnovská, R., Ulrichová, J., and Vostálová, J. (2012). DNA damage after acute exposure of mice skin to physiological doses of UVB and UVA light. Arch. Dermatol. Res. *304*, 407–412.

Thompson, M.L., McGill, T.E., McIntosh, S.M., and Manning, A. (1976). Effects of adrenalectomy on the sexual behaviour of castrated and intact BDF1 mice. Anim. Behav. *24*, 519–522.

van der Meij, L., Almela, M., Buunk, A.P., Fawcett, T.W., and Salvador, A. (2012). Men with elevated testosterone levels show more affiliative behaviours during interactions with women. Proc. Biol. Sci. *279*, 202–208.

Verhaeghe, J., Gheysen, R., and Enzlin, P. (2013). Pheromones and their effect on women's mood and sexuality. Facts Views Vis. ObGyn *5*, 189–195.

Visser, J.A., de Jong, F.H., Laven, J.S.E., and Themmen, A.P.N. (2006). Anti-Müllerian hormone: a new marker for ovarian function. Reproduction *131*, 1–9.

Walf, A.A., and Frye, C.A. (2007). The use of the elevated plus maze as an assay of anxiety-related behavior in rodents. Nat. Protoc. *2*, 322–328.

Wallner, B., Windhager, S., Schaschl, H., Nemeth, M., Pflüger, L.S., Fieder, M., Domjanić, J., Millesi, E., and Seidler, H. (2019). Sexual Attractiveness: a Comparative Approach to Morphological, Behavioral and Neurophysiological Aspects of Sexual Signaling in Women and Nonhuman Primate Females. Adapt. Hum. Behav. Physiol. *5*, 164–186.

Webb, A.R., Kazantzidis, A., Kift, R.C., Farrar, M.D., Wilkinson, J., and Rhodes, L.E. (2018). Colour counts: Sunlight and skin type as drivers of vitamin D deficiency at UK latitudes. Nutrients *10*, E457.

Yang, M., Silverman, J.L., and Crawley, J.N. (2011). Automated three-chambered social approach task for mice. Curr. Protoc. Neurosci. *Chapter 8*, 26.

Yousef, H., Alhajj, M., and Sharma, S. (2020). Anatomy, Skin (Integument), Epidermis. (StatPearls).

Zhang, B., Ma, S., Rachmin, I., He, M., Baral, P., Choi, S., Gonçalves, W.A., Shwartz, Y., Fast, E.M., Su, Y., et al. (2020). Hyperactivation of sympathetic nerves drives depletion of melanocyte stem cells. Nature *577*, 676–681.

Zimmer, C., Emlen, D.J., and Perkins, A.E.H. (2016). Evolution: Making Sense of Life (Roberts).

Zinck, L., and Lima, S.Q. (2013). Mate choice in *Mus musculus* is relative and dependent on the estrous state. PLoS ONE *8*, e66064.

Zouboulis, C.C. (2004). The human skin as a hormone target and an endocrine gland. Hormones (Athens) *3*, 9–26.

STAR★METHODS

KEY RESOURCES TABLE

REAGENT or RESOURCE	SOURCE	IDENTIFIER
Antibodies		
Anti-p53 antibody [PAb 240]	abcam	Cat #ab26; RRID:AB_303198
Anti-mouse IgG, HRP-linked	Cell Signaling Technology	Cat #7076; RRID:AB_330924
Anti-actin antibody	Sigma Aldrich	Cat #A2066; RRID:AB_476693
Anti-Rabbit IgG, HRP-linked	abcam	Cat #ab6721; RRID:AB_955447
Biological samples		
Human blood plasma	Separated from blood samples in our lab (This study)	Approval of Tel Aviv University Ethics Committee
Mouse tissue samples	Tissues obtained after sacrifice in our lab (This study)	IACUC permit#10-16-078
Chemicals		
TRIzol	Invitrogen	Cat# 15596026
Choloroform	Bio-Lab	Cat# 3082301
2-Propanol	Sigma Aldrich	Cat #278475
Methanol	Bio-Lab	Cat #136806
Paraformaldehyde, 16%	Electron Microscopy Sciences	Cat #30525-89-4
Difco Skim Milk	Avantor Sciences	Cat #90002-594
Hematoxylin Solution, Harris Modified	Sigma-Aldrich	Cat #HHS16
Eosin Y solution	Sigma-Aldrich	Cat #HT110232
DPX Mountant for histology	Sigma-Aldrich	Cat #06522
Ketamine hydrochloride	Bremer Pharma GMBH	N/A
SEDAXYLAN	Eurovet animal health	N/A
Isoflurane, USP Terrell™	Piramal Critical care, Inc.	N/A
Critical commercial assays		
Mouse LH(Luteinizing Hormone)	Wuhan Fine Biotech Co., Ltd	Cat # EM1188
Mouse GnRH(Gonadotropin Releasing Hormone)	Wuhan Fine Biotech Co., Ltd	Cat # EM1616-CM
Mouse FSH(Follicle-stimulating hormone)	Wuhan Fine Biotech Co., Ltd	Cat # EM1035
Testosterone	abcam	Cat # ab108666
Deposited data		
Raw Mass Spectrometry Data Files	This study	The mass spectrometry proteomics data have been deposited to the ProteomeXchange Consortium via the PRIDE (Perez-Riverol et al., 2019) partner repository with the dataset identifier Database:PXD025973
Experimental models: Organisms/strains		
Mouse: C57BL/6J	Envigo	N/A
Mouse: C57BL/6J-p53flx/flx	A gift from Dr. Eli Pikarsky, The Hebrew University of Jerusalem, Israel	N/A
Mouse: C57BL/6J-k14Cre+/−	A gift from Dr. Ittai Ben-Porath, The Hebrew University of Jerusalem, Israel	N/A
Mouse: p53flx/flxK14Cre−/− (Control littermates)	Bred & genotyped in our lab (This study)	N/A
Mouse: p53flx/flxK14Cre+/+ (p53-KO littermates)	Bred & genotyped in our lab (This study)	N/A

(Continued on next page)

Continued

REAGENT or RESOURCE	SOURCE	IDENTIFIER
Oligonucleotides		
See Table S5 for RT-qPCR primers	Intergrated DNA Technologies (IDT)	N/A
See Table S5 for genotyping primers	Jackson laboratories	N/A
Software and algorithms		
EthoVision XT 7	Noldus information technology	https://www.noldus.com/ethovision-xt; RRID:SCR_000441
UltraVox XT system	Noldus information technology; version 3.1	N/A
SPSS Statistics	IBM; version 25.0	https://www.ibm.com/uk-en/analytics/spss-statistics-software; RRID:SCR_002865
Prism	Graphpad; version 8	http://www.graphpad.com/; RRID:SCR_002798
Ingenuity Pathway Analysis	QIAGEN	https://digitalinsights.qiagen.com/; RRID:SCR_008653
Proteome Discoverer 1.4	Thermo Fisher Scientific	https://www.thermofisher.com/order/catalog/product/IQLAAEGABSFAKJMAUH; RRID:SCR_014477
MaxQuant	Cox and Mann, 2008; version 1.5.2.8	https://www.biochem.mpg.de/5111795/maxquant/; MaxQuant, RRID:SCR_014485
Perseus software	Cox and Mann, 2008; version 1.6.10.43	https://www.biochem.mpg.de/5111810/perseus
BioMart	Ensembl	https://www.ensembl.org/biomart/martview/9b0f3136bd9d6999b66c3a766729a6ae
Other		
Virusolve®+	Amity International	N/A
Veet hair removal cream	Reckitt	N/A
UVB Lamp (Model: XX-15MR Bench Lamp, 302 nm)	Analytik Jena US	Cat # 95-0042-15
UVX radiometer	Analytik Jena US	Cat #97-0015-02

RESOURCE AVAILABILITY

Lead contact
Further information and requests for resources and reagents should be directed to and will be fulfilled by the Lead Contact, Carmit Levy (carmitlevy@post.tau.ac.il).

Materials availability
All in-house generated mouse strains generated for this study are available from the Lead Contact with a completed Materials Transfer Agreement.

Data and code availability

- All original datasets has been deposited at the ProteomeXchange Consortium via the PRIDE (Perez-Riverol et al., 2019) partner repository and is publicly available as of the date of publication: Database: PXD025973.
- This paper does not report original code.
- Any additional information required to reanalyze the data reported in this paper is available from the lead contact upon request.

EXPERIMENTAL MODEL AND SUBJECT DETAILS

Mouse models and habituation
Unless stated otherwise, we used 5- to 6-week-old C57BL6 male and female mice (Envigo) for experiments. The p53 floxed male and female mice were a gift from Dr. Eli Pikarsky (The Hebrew University of Jerusalem, Israel). Dr. Ittai Ben-Porath (The Hebrew University

of Jerusalem, Israel) provided male and female mice in which the *K14* promoter directs expression of Cre recombinase. We confirmed the *p53* knockout in keratinocytes by genotyping, qRT-PCR, and ear pigmentation analysis. Male and female mice were habituated for at least 1 week to their new environment under a standard 12-h light/dark cycle and the conditions of constant temperature ($24 \pm 1°C$) and humidity ($50 \pm 5\%$) with access to food and water *ad libitum* prior to experimentation. The guidelines of the Tel Aviv University Institutional Animal Care and Use Committee (IACUC) (10-16-078) were followed.

Human cohort
The human cohort of 9 men and 10 women (18-55 year of age) were recruited through convenience sampling at the Sackler School of Medicine (Tel Aviv University, Israel). All provided written consent. The approval of the University's Ethics Committee was obtained prior to the study.

Human cohort testosterone study
The human cohort study from Clalit was approved by Kaplan Medical Center Institutional Review Board. Total testosterone data and related medical data were retrieved for all males aged 20 to 50 years old in Israel Central and Jerusalem districts from Clalit Health Services using Clalit Secure Data Sharing Platform powered by MDClone (https://www.mdclone.com), and subjects with testosterone modifying medical conditions were excluded. Subjects were classified into four groups categorized according to average UV radiation (UVR) in their country of origin (https://apps.who.int/gho/data/node.main.164?lang=en) by using WHO map (https://www.who.int/gho/phe/ultraviolet_radiation/exposure/en/). Only men from countries with low UVR (UV < 2500 J/m^2) and high UVR (UV $\geq$ 4500 J/m^2) were considered for this study. Multivariate analysis of variance models was used to estimate the effect of seasonality and country of origin on total testosterone levels. Models were assessed separately for the summer (May-September) and winter (October-April) months and were adjusted for age and body mass index. The analysis of human cohort testosterone level data of men aged 21-25 years old (n = 13,086) from the Maccabi Health Services, was done as previously described (Chodick et al., 2020).

Human questionnaire
For the quantitative longitudinal study, 19 subjects aged 23–73 (mean M = 45.89, SD = 15.22), 47.4% male and 52.6% female, with skin conditions including vitiligo, eczema, and psoriasis were recruited by convenience sampling from two Israeli hospitals (Assuta Hospital; Helsinki ethical approval 0063-17-ASMC 17 and Tel Aviv Sourasky Medical Center; Helsinki ethical approval 0151-17-TLV). Of all the participants, 11.8% were single, 64.7% were married, and 23.5% were divorced, 35.3% had no children, and 64.7% had 1–3 children. Data were collected through self-reported questionnaires at two time points, before exposing the participants to a UVB treatment (T1), and approximately a month after the treatment (T2). During this period, patients were given full body (except their genitals, eyes, and head) narrow band UVB exposure (0.1-2.5 J/cm) (Waldmann UV7002 UVB instrument; UV lamp (UVB) 42 x TL 01 120 W) 2-3 times a week, 10-12 UVB exposures in total. The hospitals IRB approved the study, and all participants signed informed consent forms.

The PLS (Hatfield and Sprecher, 1986) was developed to measure passionate love in intimate relationships and focuses on an intense longing for union with the other. We used a Hebrew translation of the PLS for our study. We used seven items from the short version of the PLS relevant to our study: cognitive components of passion (intrusive thinking about the partner, idealization of the other and the relationship); emotional components of passion (attraction, longing for reciprocity, and physiological arousal). From the short version of the PLS, we excluded items that did not directly examine the person's passion, such as actions taken to determine the other person's feelings. We included items related to cognitive components of passion (e.g., intrusive thinking about the other and idealization of the other and the relationship) and emotional components of passion (e.g., attraction, longing for reciprocity, and physiological arousal). Each item was rated on a 9-point Likert-scale (1 = not at all true; 9 = definitely true), with a higher score representing more passionate love.

The aggression questionnaire (Buss and Perry, 1992) was developed to measure four aspects of aggressiveness: physical aggression, verbal aggression, anger, and hostility. A questionnaire translated into Hebrew was used to assess two factors relevant to our study: physical aggression (nine items; e.g., 'I get into fights a little more than the average person') and verbal aggression (five items; e.g., 'I can't help getting into arguments when people disagree with me'). Each factor was rated on a 5-point Likert-scale (1 = extremely uncharacteristic of me; 5 = extremely characteristic of me) and calculated by summing the answers (after re-coding one item of physical aggression), with higher scores representing more aggression. The reliability of the scale of the original questionnaire, measured through Cronbach's alpha, was 0.85 for physical aggression and 0.72 for verbal aggression. In our study, the Cronbach's Alpha was 0.84 in T1 and 0.77 in T2 for physical aggression (after deleting one item); and 0.81 and 0.79, respectively, for verbal aggression.

METHOD DETAILS

UV treatment
Mice were kept in a reverse 12-h dark/light cycle (red light) and were shaved on the dorsal side in an area of approximately ~60% of the skin, excluding the ears, tail and paw regions, where hair growth is not prevalent, and were treated with depilatory cream (Veet). Mice were exposed to daily UVB treatment of 50 mJ/cm^2 in the reverse light setting with a XX-15 stand equipped with 15-W, 302-nm

UVB bulbs (Ultraviolet Products) at approximately the same time of their day (9:00 – 10:00 AM) in a custom transparent plexiglass chamber that allowed freedom of movement during the treatment. To exclude the possibility of not crawling on top of each other and hindering the UVB skin exposure, one mouse per chamber at a time were UVB exposed (Nghiem et al., 2002). The UV emission was measured using a UVX radiometer (Ultraviolet Products, 280 nm – 320 nm) equipped with a UVB measuring head. The calibration was done for the delivered doses of UVB emission. For the mock (control) treatment, the animals were placed in the chamber but the UVB lamp was not turned on, which ensured that the UVB-exposed and control mice experienced the same stress conditions. After each treatment, the container was cleaned using Virusolve (Amity International) to avoid cross-contamination of odors. Control and UVB exposed mice used for the study were of similar age and underwent similar experimental protocols in order to exclude the possibility of hair-cycle differences as well as stress related interferences in the behavioral experiment.

Melanin intensity quantification

The reflective colorimetric measurements were performed with a DSM II Color Meter (Cortex Technology), which gives the level of pigmentation. A white standard background (provided by the manufacturer) was used for the calibration before every measurement. All the measurements were performed on the same background with no UV light. The tail and ear pigmentation were measured at the end of the 8-week UVB (50 mJ/cm^2) or mock (control) treatment series and at the end of 5-week period for p53-KO and p53-WT animals, and pigmentation intensity was scored relative to control (UV/Mock - melanin pigmentation intensity).

Mouse blood draw

Mice were anesthetized by the intraperitoneal injection of ketamine (100 mg/kg body weight; Bremer Pharma GMBH) and xylazine (10 mg/kg body weight; Eurovet Animal Health BV), and blood was drawn from the heart with a 23G needle (KDL) at approximately the same time of the day (between 10:00 – 13:00 Israel Standard Time) for all samples. The drawn blood was transferred to EDTA-coated microvette tubes (BD Mictrotainer) and immediately placed on ice, followed by centrifugation at 448 g for 10 min at $4°C$ to separate the plasma fraction, which was then aliquoted and stored at $-80°C$ until further use.

Human cohort Solar-exposure study

All subjects were asked to avoid or minimize their solar exposure during the 2 days prior to the experiment and were requested to wear long-sleeved clothes on those days. On the day of the experiment (between 16:00-18:00, Israel standard time), 10 cc of intravenous blood was drawn by a certified physician. On the next day subjects were asked to wear short sleeves/sleeveless shirt and shorts and be in a non-shaded area in order to expose themselves to 2000 mJ/cm^2 solar UV radiation, as measured by the UVX radiometer (Ultraviolet Products, 280 nm – 320 nm), between 11:00-13:00, Israel standard time. The second blood sample was then drawn later that day, between 16:00-18:00, Israel standard time.

Human blood draw

Venous blood was drawn from the forearm, after disinfection with Alcosept (chlorhexidine gluconate 0.5% W/V and alcohol 70% V/V; Floris) using a blood-collecting needle set (KDL). Blood was collected in Vacutainer® tubes (BD Biosciences). The blood was allowed to clot at room temperature for 15-30 min followed by centrifugation at 2000 g for 10 min at $4°C$ to separate the serum fraction, which was then aliquoted and stored at $-80°C$ until further use.

Proteolysis and mass spectrometry

Proteins from plasma of five human volunteers randomly selected from the cohort and from three mice were precipitated with 90% ethanol at $90°C$ for 10 min, followed by centrifugation at 11,200 g for 5 min. The resulting supernatant was dried and resuspended in 9 M urea, 400 mM ammonium bicarbonate, reduced with 3 mM DTT ($60°C$, 30 min), modified with 12 mM iodoacetamide in 400 mM ammonium bicarbonate (in the dark, at room temperature, 30 min), and digested in 1 M urea, 50 mM ammonium bicarbonate with modified trypsin (Promega) at a 1:50 enzyme-to-substrate ratio at $37°C$ for 2 h. The tryptic peptides were desalted using C18 tips (Top tip, Glygen), dried, and re-suspended in 0.1% formic acid. The peptides were then resolved by reverse-phase chromatography on 0.075 X 180 mm fused silica capillaries (J&W Pharmalab) packed with Reprosil reversed-phase material (Dr Maisch GmbH). The peptides were eluted with a linear 60-min gradient from 5% to 28%, then a 15-min linear gradient from 28% to 95%, followed by 25 min at 95% acetonitrile with 0.1% formic acid in water, at a flow rate of 0.15 µl/min. Mass spectrometry was performed with a Q Exactive HF mass spectrometer (Thermo Fisher Scientific) in a positive mode, using repetitively full MS scan followed by collision induced dissociation of the 18 most dominant ions selected from the first MS scan. The mass spectrometry data from three biological repeats was analyzed using the MaxQuant software 1.5.2.8 (Cox and Mann, 2008). The data was quantified by label-free analysis using the same software. Statistical analysis of the identification and quantization results was done using Perseus 1.6.10.43 software (Cox and Mann, 2008).

Proteomic analysis

The proteomic dataset, which included the UniProt identifiers, were converted to gene symbols using BioMart, Ensembl. The gene symbols and absolute value of the $\log_2$-transformed fold-change were subjected to IPA for the core analysis (QIAGEN). Matching with the mouse Ingenuity Knowledge Database generated predicted possible upstream and transcription regulators based on the p value and

activation Z-score values, which infers the activation state (increased or decreased). Fisher's right-tailed exact test was used to determine the probability of upstream analysis over-representation in the dataset. The protein network was built using the string output.

ELISA

Testosterone, LH, FSH, and GnRH levels in mouse plasma were detected and quantified after 8 weeks of UVB (50 mJ/cm^2) or control treatment using the Testosterone Elisa Kit (ab108666, Abcam), LH Elisa kit (EM1188, Wuhan Fine Biotech Co., Ltd.), FSH Elisa kit (EM1035, Wuhan Fine Biotech Co., Ltd.), and GnRH Elisa Kit (EM1616-CM, Wuhan Fine Biotech Co., Ltd.), according to the manufacturers' instructions.

Mating test

<u>Procedure</u>: This test was conducted on sexually naive female and male C57BL6, p53-WT, and p53-KO mice after UVB (50 mJ/cm^2) or mock treatment. The males were individually housed for 24 h in a new cage with sawdust bedding; food and water were provided *ad libitum*. Before the start of the mating test, the food and water were removed from the cage, and the females were examined for the stage of their estrous cycle; they were mated with a male only if they were in the estrus/proestrus stage. In the mating test, a female was introduced into the cage of the male, where she spent 1 hour, after which she was immediately returned to her cage. All tests were conducted in a 17 × 25 cm transparent plexiglass chamber placed on a table that allowed videotaping in the ventral view with a digital camera. The visual data were subsequently analyzed manually for respective behavior parameters. All the experiments took place in a reverse 12-h light/dark cycle under dim, red lighting. In the case of the p53-WT and p53-KO mice, the mating test was carried out at the end of the light phase of the standard 12-h light/dark cycle under dim, red lighting, as mating behavior was tested during the active phase (dark phase) of the mice.

<u>Analysis parameters and criteria</u>: The following parameters were measured as previously described (Haga et al., 2010): number of anogenital sniffs, grooming behavior, latency and total number of male mounting of the female, intromission latency, duration and total number of intromissions, female lordosis response, rearing behavior, and number of ejaculations. *Anogenital sniffing* was defined as actively reaching out and sniffing the genital regions of a mouse. *Reaching out* was defined as a mouse trying to stretch out and sniff the other sex's genitalia. *Mouse grooming behavior* was scored when the mouse self-groomed its face or body. *Mounting* was defined as a failed attempt of the male to climb with both forepaws on the female's back in an attempt to mate. *Intromission* was defined as a male successfully climbing on the female with its forepaws and making pelvic thrust movements with a stable frequency for a minimum duration of 5 s. A female's *lordosis response* was defined as the female standing on all four paws grounded and elevating the hind region from the floor, creating a lordotic curve of the spine. A female was classified as receptive only if she exhibited the lordotic posture upon mounting by a male. The lordosis analysis was performed against the total number of mounting with pelvic thrusts by male mouse, which may or may not include penile intromission (Lordosis quotient = Total number of female lordosis/total number of male mounts*100) in a single experimental session as previously described (Beach, 1976; Haga et al., 2010). *Rearing* behavior was considered a female assuming a defensive upright posture toward a male, with both forepaws in the air and the back straight and stretched. *Ejaculation* was defined as the end of the intromission period, when the male, after ejaculating, would fall on one side and remain in that position for a couple of seconds.

Ultrasonic vocalization

Sexually naive male and female mice were subject to the above-described mating test but in a room suited for recording their ultrasonic vocalizations. Recordings were obtained using an UltraVox XT system (Noldus Information Technology), which was capable of recording the full spectrum of sound with a maximum frequency of 160 kHz. Detector outputs were analyzed with UltraVox XT 3.1 software (Noldus Information Technology). The number of vocalizations, mean dominant frequency, duration of the mice vocalizing with each other was recorded and scored. A representative spectrogram of the vocalization was extracted using the UltraVox XT 3.1 software.

Elevated plus maze test

The elevated plus maze test was performed after 5 weeks of UVB or control treatment with an apparatus measuring 90.0 cm in height made of white plexiglass. The maze consisted of four arms in total (two open arms without walls and two enclosed arms with 15.0-cm high walls). The mice were habituated for 30 min to the experimental room prior to the start of experiment in order to avoid the stress bias of a new environment. Naive mice, who did not undergo any experimental protocols other than the UVB and control treatments were used for this study thus giving us the true measure of the test unhindered from the stress due to other behavioral experiments. The control or UVB-treated mouse was placed in the center of the maze (intersection of the open and closed arms) facing the open arm and was allowed to move for 7 min in the maze. The mouse behavior was recorded in a digital video camera mounted overhead on the ceiling and was scored and analyzed using the Ethovision XT software (Noldus Information Technology). The test was conducted in a reverse 12-hour light/dark condition under the dim red light setting during their active phase cycle. The females were checked for their estrous cycle by vaginal smears prior to the experiment in order to avoid the bias of the state of the cycle influencing the anxiety parameter. Between each trial, the maze was cleaned using Virusolve (Amity International) to avoid cross contamination of odors between gender and treatments. The parameters scored included the total time spent giving the cumulative of the time spent either in the open or closed arm and the frequency giving the number of visits by the mouse either in the open or closed arms of the elevated plus-maze.

Three-chamber test

A white, rectangular, plexiglass chamber was divided into three consecutive compartments, with each of the two outer compartments containing a wire cage. Small openings in the center of the two partitions facilitated movement throughout the chamber, except into the wire cages. The wire cage limits movement of the stimulus mouse. To habituate the subject mouse to the test chamber, it was placed in the center of the middle chamber with freedom of movement on either side of the compartment for 10 min the day before the experiment; no stimuli was introduced. On the day of the experiment, the subject and stimulus mice were brought into the experimental room and habituated to the room for 20 min. Next, the stimulus mice (or novel objects) were placed in the wire cages, one in each cage. The subject mouse was then placed in the center of the middle compartment and allowed to move freely for 15 min. The experiments were performed under a reverse 12-h light/dark phase under dim, red lighting. A digital camera mounted overhead on the ceiling was used to record the mouse's behavior throughout the 15-min session, which was scored using EthoVision XT software (Noldus Information Technology). Between each trial, the positions of the stimuli were switched, to avoid a confounding error (preferred side of the subject mouse), and the chamber and wire cages were cleaned using Virusolve (Amity International), to avoid cross-contamination of the odors from the subject or the stimulus mice.

The coordinates and time stamps of the subject mouse obtained from a live video feed were translated into a number of parameters and further visualized by a heatmap generated with EthoVision XT software (Noldus) to detect the subject mouse's location and movements. We scored the following parameters: latency toward the zone of the cage and near the cage, which are the amounts of time taken by the subject mouse to move toward a compartment with a stimulus. The total time spent in the zone of the cage and near the cage represents the cumulative time spent in the compartment with a stimulus. The frequency of visits to the zone of the cage and near the cage provides the number of times the subject mouse visited a compartment with a stimulus.

In all the following schemes, mice received UVB (50 mJ/cm^2) or control treatment for 5 weeks. All the female mice were examined prior to the test session for their estrous cycle stage, with only those in their estrus/proestrus stage used in the test.

Male subject and two female stimuli

The same stimulus females (one UVB-treated and one control female) were tested twice, once with a control male mouse subject and once with a UVB-treated male mouse subject, on separate days.

Female subject and two male stimuli

The same stimulus males (one UVB-treated and one control male) were tested twice, once with a control female subject and once with a UVB-treated female subject, on separate days.

Female subject and two female stimuli

The same stimulus females (one UVB-treated and one control female) were tested twice, once with a control female subject and once with a UVB-treated female subject, on separate days.

Female subject, a male stimulus, and a novel-object stimulus

The same stimulus male (one set of experiments with a UVB-treated male and the other with a control male) were tested twice, once with a control female mouse subject and once with a UVB-treated female mouse subject, on separate days. The novel object (plastic block) was cleaned using Virusolve (Amity International) between each trial.

Vaginal smears for estrous cycle evaluation

To examine the estrous cycle, a gentle lavage technique was used to collect vaginal smears from each female mouse daily, approximately at the same time, for a period of 45 days, starting when the females were 4 weeks old. In the first 2 weeks of smear collection, females were not subject to any treatment. In the following 4 weeks, the females were subjected UVB (50 mJ/cm^2) or control treatment.

The smear collection involved gently inserting a 200-μl pipette tip containing 30 μl sterile PBS X1 into the vagina to a depth of 3 mm, and the lavage was smeared onto a plain glass slide (76 × 26 mm, Bar Naor Ltd.). The smears were then immediately viewed under a bright field microscope (Nikon) to assess the stage of estrous cycle, as determined by examining the morphology of the cells present in the vaginal smear, as described previously (Caligioni, 2009). The proestrus stage was characterized by the presence of nucleated epithelial cells; the estrus stage by enucleated cornified cells; the metestrus stage by leucocytes, cornified cells, and nucleated epithelial cells; and the diestrus stage by the predominant presence of leucocytes and lower amounts of nucleated cells. For Figure 3B, the proestrus and estrus stage were combined and the diestrus and metestrus stage were combined as previously done (Ajayi and Akhigbe, 2020) for the subsequent analysis.

RNA purification and qRT-PCT

Flash-frozen tissues were thawed on ice, followed by homogenization with magnetic beads of the desired size (Next Advance) in a Bullet Blender (Next Advance). Total RNA was purified using TriZol (Invitrogen) according to the manufacturer's guidelines. RNA was quantified by measuring the OD$_{260\,nm}$/OD$_{280\,nm}$. For the mRNA analysis, the cDNA was prepared using the qScript cDNA synthesis kit (Quantabio) and further subjected to qRT-PCR using PerfeCTa SYBR green FastMix (Quantabio). The data are represented as the

fold changes relative to the control. All experiments were performed at least in triplicates. All the primer sequences used are presented in Table S5.

Histology

Following UVB or control treatment of female mice, the ovaries were fixed in 4% paraformaldehyde and paraffin-embedded, followed by staining with hematoxylin (HHS16, Sigma-Aldrich) and eosin (HT110232, Sigma-Aldrich) according to the manufacturer's instructions. Sections of 5 μm were mounted using the DPX mountant (06522, Sigma-Aldrich). The images were obtained with an Aperio Slide Scanner microscope (Leica Biosystem, USA), at × 20 magnification.

Genotyping

Genomic DNA was extracted from the tail of a mouse using extraction buffer (25 mM NaOH, 0.2 mM disodium salt EDTA; pH 12) for 60 min, followed by incubation in neutralization buffer. PCR was performed in a 20-μl volume that included 10 μl GoTaq green master mix (× 2) (Promega), 0.5 μM Cre primers (with positive control) and 0.5 μM flox primers (Integrated DNA Technologies). Reactions were carried out in a PCR cycler (Biometra PCR Cycler) at 95°C for 3 min, followed by 35 cycles at 95°C for 30 s, a cycle at 55°C for 1 min, and an extension step at 72°C for 5 min. The PCR products were kept at 4°C until electrophoresis in 3% agarose gel. The visualization of the PCR product was done based on its size (Cre-recombinase 100 bp, internal positive control 324 bp, flox 390 bp), and the digital images were captured in a Gel Documentation system (UVITEC Ltd.).

Immunoblotting

Whole skin tissues were dissected from mice and snap frozen in liquid nitrogen followed by homogenization in RIPA buffer with protease inhibitor (Roche) as previously described (Glaich et al., 2019). This was followed by incubation on ice for 1 hour, then the samples were centrifuged at 10,000 g for 15 mins at 4°C. The resulting clear phase protein was stored at −80°C until further use. Samples were subjected to western blot analysis as described previously (Dror et al., 2016). Membrane was exposed overnight to antibody targeting p53 (ab26, Abcam) and Actin (#A2066, Sigma Aldrich) and proteins were visualized with SuperSignal Chemiluminescent Substrates (Pierce) using horseradish peroxidase-conjugated anti-mouse antibody (#7076, Cell Signaling) and horseradish peroxidase-conjugated anti-Rabbit antibody (#ab6721, abcam). The p53 protein levels in each condition were normalized to actin (Q).

QUANTIFICATION AND STATISTICAL ANALYSIS

The data are shown by means and standard errors. We performed two-tailed Student's t tests for two group comparisons and ANOVA for multiple group comparisons. For the PLS questionnaire, we used IBM SPSS (version 25.0) and conducted Wilcoxon tests to examine within-group differences (ranks of T1 versus T2 for each gender separately). For all the tests, p values < 0.05 were considered significant. All the analyses were performed using Excel (Microsoft Corp.), SPSS (version 25.0), and GraphPad PRISM 8 software. The statistics details and the software's used for all the experiments can be found in the resources tables and figure legends and the Human questionnaire statistics details can be found in the STAR Methods section: Human questionnaire.